ACKNOWLEDGEMENTS

Agradeço à Professora Susana Pereira e ao Professor José Pissarra, pela oportunidade e confiança depositada. Pelo apoio e dedicação constantes, pelo entusiasmo e por todo o conhecimento partilhado. Obrigada.

Agradeço ao fantástico grupo do 2.61! Ao Alberto, ao Bruno e à Vanessa, pelas conversas sérias e pouco ou nada sérias, pelos sorrisos e risadas, pelo apoio constante, pela ajuda e companheirismo, que desde o primeiro dia me fizeram sentir em casa.

Um agradecimento muito especial à Cláudia. Pela dedicação e apoio incansáveis, mesmo que fosse pelo telefone, mensagem, email ou pombo correio, e mesmo quando tudo parecia impossível! Obrigada pela (muita) paciência, pela persistência e por acreditares sempre, até quando as coisas corriam menos bem. Obrigada!

A ti, Gabriel, obrigada por seres o meu porto seguro. Obrigada por tudo, sempre.

À minha família, o meu berço, obrigada pelo apoio incondicional.

Aos meus pais, o meu agradecimento mais doce. São a fonte de toda a minha força e sem eles com certeza não teria chegado até aqui.

SUMMARY

In the past few years, the plant cell wall has been drawing more and more attention from the scientific community, particularly regarding the protein trafficking to and from this compartment. The secretion of soluble proteins has been for a long time thought to occur by bulk flow, following a *default* pathway to the extracellular matrix. However, data has been emerging on the possibility of the sorting to the cell wall is in fact regulated somehow, despite the absence of identified signals or receptors. Endocytic routes have also been suggested to be involved in the regulation of protein sorting to and from the cell wall. Moreover, the biogenesis of the cell wall itself depends on numerous intracellular trafficking and secretion events and it has been shown that those events are most probably controlled specifically and rigorously by the cell wall. From this perspective, as a vital compartment of the plant cell and holding a strategic position between the cell and the environment, the cell wall could in fact control and regulate certain cargo trafficking inside the cell, as well as important secretion events.

Cardosin A and cardosin B are aspartic proteinases first isolated from the flower tissues of cardoon (*Cynara carduculus* L.), which have been thoroughly characterised in our group. When transiently expressed in *Nicotiana tabacum* leaves, both cardosins have shown to accumulate in the lytic vacuole. Recently, however, experiments were conducted in *N. tabacum* mesophyll protoplasts and, curiously, cardosin B showed to be secreted to the culture medium, which could point towards a regulation by the cell wall. Moreover, the vacuole sorting determinants recently identified for cardosins – C-terminal peptides and the PSI domain – which are also worth investigating for a possible role in the regulation of sorting by the cell wall. The PSI from cardosin A, in particular, for the intriguing capability of directing proteins to the vacuole through a Golgi-independent route, seemed worth exploring in more detail.

Taking together the results of this study, the hypothesis of a role for the plant cell wall in the regulation of protein trafficking appears as plausible. The absence of cell wall in *N. tabacum* protoplasts expressing cardosins, which are typically vacuolar in this system, have originated partial protein secretion. The same pattern was observed for C-terminal peptides, which are known to follow the same intracellular route as whole cardosins; however, no secretion was detected for PSI A, supporting the Golgi-independent proposed route before reaching the lytic vacuole. As a whole, this study enhances the dynamic and active role of the cell wall in the protein sorting events and is the starting point of several studies exploring its participation on the regulation of intracellular sorting.

RESUMO

Nos últimos anos, a parede celular das plantas tem vindo a atrair a atenção da comunidade científica, particularmente no que diz respeito ao trânsito de proteínas de e para este compartimento. A secreção de proteínas solúveis foi considerada durante muito tempo como uma via *default*, transportando as proteínas para a matriz extracelular. Contudo, tem sido sugerida a possibilidade do transporte para a parede celular ser de facto regulado, apesar da inexistência de sinais ou recetores identificados. A via do endossoma é sugerida como estando envolvida na regulação do trânsito de proteínas de e para a parede celular. Por outro lado, a biogénese da própria parede celular depende de inúmeros processos de trânsito intracelular e secreção, e tem vindo a ser sugerido que estes são presumivelmente controlados pela parede celular de forma específica e rigorosa. Assim, sendo um compartimento vital à célula vegetal e detendo esta uma posição estratégica entre a célula e o meio exterior, a parede celular poderá de facto controlar e regular determinados transportes intracelulares de proteínas, assim como processos relevantes de secreção.

A cardosina A e a cardosina B são proteinases aspárticas que foram isoladas pela primeira vez dos tecidos da flor de cardo (*Cynara cardunculus* L.), e têm sido extensivamente caracterizadas no nosso grupo. Quando expressas de forma transiente em folhas de *Nicotiana tabacum*, ambas demonstraram acumular-se no vacúolo lítico. Recentemente, porém, foram efetuados estudos em protoplastos do mesófilo de *N. tabacum* e, curiosamente, verificou-se que a cardosina B era secretada para o meio de cultura, o que aponta para uma regulação por parte da parede celular. Recentemente, foram ainda identificados os determinantes vacuolares das cardosinas – a região C-terminal e o domínio PSI – cujo possível papel da parede celular na regulação do trânsito é também motivo de interesse. O PSI da cardosina A, em particular, pela sua intrigante capacidade de direcionar proteínas para o vacúolo por uma via independente do complexo de Golgi, suscitou especial interesse para um estudo mais detalhado.

De acordo com os resultados obtidos no presente estudo, a hipótese de a parede celular ter um papel na regulação do transporte de proteínas surge como plausível. A ausência de parede celular em protoplastos de *N. tabacum* a expressar cardosinas, tipicamente vacuolares neste sistema, originou a secreção parcial destas proteínas. O mesmo padrão é observado para os péptidos C-terminal, cuja rota intracelular é semelhante à das cardosinas; contudo, não foi observada secreção para o PSI A, suportando a rota para o vacúolo independente do complexo de Golgi. Em suma, este estudo realça o papel dinâmico e ativo da parede celular em processos de trânsito proteico e poderá ser um ponto de partida para diversos estudos, nomeadamente a exploração da sua participação na regulação do trânsito intracelular.

TABLE OF CONTENTS

ACKNOWLEDGEMENTS 1
SUMMARY 3
RESUMO 5
TABLE OF CONTENTS 7
LIST OF TABLES 11
LIST OF FIGURES 13
1. INTRODUCTION 19
1.1. The Endomembrane System 20
1.1.1. The Endoplasmic Reticulum 21
1.1.2. The ER – Golgi Interface 22
1.1.3. The Golgi apparatus 24
1.1.4. Post-GA transport 24
Protein Trafficking to the Vacuoles 25
Protein Trafficking to the Cell Wall 27
1.2. Cardosins – Models for Protein Sorting Studies 28
Cardosins – Aspartic Proteinases 28
Cardosins and Protein Sorting 29
1.3. Objectives of the Thesis 31
2. METHODOLOGY 32
2.1. Dissecting the role of the plant cell wall in the regulation of protein trafficking. 33
2.1.1. Germination and maintenance of *Nicotiana tabacum* SRI cv. Petit Havana 33
2.1.2. Isolation of protoplasts from *Nicotiana tabacum* leaves 33
2.1.3. Cell wall regeneration in *Nicotiana tabacum* protoplasts 33
2.1.4. Infiltration of *Nicotiana tabacum* leaves 34
2.1.5. Secretion assays 34
2.1.6. Protein extraction from protoplasts 36

2.1.7. Preparation of proteins from protoplasts' culture medium by Trichloroacetic acid (TCA) precipitation 36
2.1.8. SDS-PAGE and Western blotting 36
2.1.9. Fluorescence Microscopy and Confocal Laser Scanning Microscopy 37
2.2. Unveiling the role of the PSI domain in the regulation of cardosin A trafficking 38
2.2.1. Primers design and site-directed mutagenesis 38
2.2.2. Addition of restriction enzyme adaptors 41
2.2.3. Cloning into pCR-Blunt vector 42
2.2.4. Plasmid miniprep and enzymatic restriction screening 42
2.2.5. Sub-cloning into pVKH18-En6 43
2.2.6. Transient expression in *Nicotiana tabacum* 43
2.2.7. Expression analysis by CLSM 44
2.3. Maintenance and transformation of bacterial strains used along the work 44
2.3.1. Preparation of competent *Escherichia coli* 44
2.3.2. Transformation of *Escherichia coli* 45
2.3.3. Preparation of electrocompetent *Agrobacterium tumefaciens* 45
2.3.4. Transformation of *Agrobacterium tumefaciens* 45
3. RESULTS 46
3.1. Dissecting the role of the plant cell wall in the regulation of protein trafficking 47
3.1.1. Protoplast culture and cell wall regeneration optimisation 47
3.1.2. Analysis of cardosins' trafficking during protoplasting and cell wall regeneration 50
3.1.3. The role of C-terminal region in cardosins trafficking during protoplasting and cell wall reforming 54
3.1.4. The role of PSI domain in cardosins trafficking during protoplasting and cell wall reforming 57

3.2. Unveiling the role of the PSI domain in the regulation of cardosin A trafficking 62

4. DISCUSSION 66

4.1. Dissecting the role of the plant cell wall in the regulation of protein trafficking 67

N. tabacum protoplasts regenerate a cell wall as early as 24h upon isolation 67

Cardosins A and B became secreted upon protoplasting 68

The C-terminal VSD is responsible for cardosins secretion during protoplasting 71

The PSI:mCherry constructs are not secreted upon protoplasting 72

4.2. Unveiling the role of the PSI domain in the regulation of cardosin A trafficking 73

5. CONCLUSIONS AND FUTURE PERSPECTIVES 75

6. BIBLIOGRAPHIC REFERENCES 78

LIST OF TABLES

Table 1 - Primers used in the Site-directed mutagenesis of cardosin A. 39

Table 2 - PCR reactions' composition used for the Site-directed mutagenesis of cardosin A. ..40

Table 3 - PCR conditions used for the Site-directed mutagenesis of cardosin A. 40

Table 4 - Primers used for the addition of restriction enzyme adaptors to AmutPSI construction. 41

Table 5 - PCR reactions' composition used for the addition of restriction enzyme adaptors to AmutPSI construction. 41

Table 6 - PCR conditions used for the addition of restriction enzyme adaptors to AmutPSI construction.....42

Table 7 - Summary of the results obtained on the secretion assays performed, comprising the observations made through CLSM and Western blotting.....61

LIST OF FIGURES

Figure 1 - Schematic representation of the cargo transport between the ER export sites and the Golgi apparatus. 22

Figure 2 - Schematic models of ER-Golgi protein transport. 23

Figure 3 - Schematic representation of soluble proteins transport to the vacuoles....26

Figure 4 - Schematic representation of the proposed sequence of events during the processing of cardosin A. 29

Figure 5 - Schematic representation of the chimeric constructions used in this study. 35

Figure 6 - Monitorisation of cell wall regeneration in *N. tabacum* protoplasts maintained in medium A. 48

Figure 7 - Monitorisation of cell wall regeneration in *N. tabacum* protoplasts maintained in medium B. 49

Figure 8 - Confocal microscopy images of *N. tabacum* mesophyll protoplasts and the respective leaf of origin, expressing cardosinA-mCherry during secretion assay and Western blot of the respective cell/medium protein fractions. 51

Figure 9 - Confocal microscopy images of *N. tabacum* mesophyll protoplasts and the respective leaf of origin, expressing cardosinB-mCherry, during secretion assay and Western blot of the respective cell/medium protein fractions. 53

Figure 10 - Confocal microscopy images of *N. tabacum* mesophyll protoplasts and the respective leaf of origin, expressing mCherry-CTermA, during secretion assay and Western blot of the respective cell/medium protein fractions. 55

Figure 11 - Confocal microscopy images of *N. tabacum* mesophyll protoplasts and the respective leaf of origin, expressing mCherry-CTermB, during secretion assay and Western blot of the respective cell/medium protein fractions. 56

Figure 12 - Confocal microscopy images of *N. tabacum* mesophyll protoplasts and the respective leaf of origin, expressing PSIA-mCherry, during secretion assay and Western blot of the respective cell/medium protein fractions. 58

Figure 13 - Confocal microscopy images of *N. tabacum* mesophyll protoplasts and the respective leaf of origin, expressing PSIB-mCherry, during secretion assay and Western blot of the respective cell/medium protein fractions. 60

Figure 14 - Agarose gel electrophoresis of plasmid miniprep obtained from site-directed mutagenesis of PSI cleavage sites. 62

Figure 15 - PCR products from restriction enzyme adaptors addition on AmutPSI_STP and AmutPSI_noSTP. 63

Figure 16 - Restriction analysis of AmutPSI_STP and AmutPSI_noSTP after insertion into pCRBlunt vector. 63

Figure 17 - Restriction analysis of the insertion of AmutPSI_STP and AmutPSI_noSTP into pVKH18-En6 vector. 63

Figure 18 - Schematic representation of AmutPSI and AmutPSICh constructions. 64

Figure 19 - Confocal microscopy images of *N. tabacum* leaves expressing AmutPSICh three and six days after agroinfiltration, and cardosinA-mCherry three days after agroinfiltration. 65

Figure 20 - Schematic representation of the cell wall influence in the sorting of cardosins.....69

Figure 21 - Schematic representation of the close proximity between the secretory and endocytic pathways.....70

LIST OF ABBREVIATIONS

µg - microgram

µL - microliter

APs – Aspartic Proteinases

B5 – Gamborg's B5 medium

BiP - Binding protein

BSA – Bovine serum albumine

BY2 – Bright Yellow 2 cells

CCV – Clathrin Coated Vesicle

CLSM – Confocal Laser Scanning Microscopy

C-ter – C-terminal peptide

ctVSD – C-terminal vacuolar sorting determinant

d - day

DNA – Deoxyribonucleic acid

dNTPs – Deoxyribonucleotides tri-phosphate

DV – Dense vesicle

EE – Early Endosome

ER – Endoplasmic reticulum

ERES – ER export sites

GA – Golgi apparatus

GFP – Green Fluorescent Protein

GTP - Guanosine-5'-triphosphate

h - Hour

kDa - Kilodalton

Kb - Kilobase

LB – Luria Bertani medium

LE – late endosome

LV – Lytic vacuole

Min - minute

mL – milliliter

mM - milimolar

MVB – Multivesicular Body

PAC – Precursor accumulating vesicles

PCR – Polymerase Chain Reaction

PDI – Protein disulfide isomerase

PM – Plasma membrane

Pre – Signal peptide present in aspartic proteinases precursor

Pro – Prosegment present in aspartic proteinases precursor

PSI – Plant Specific Insert

PSV – Protein Storage Vacuole

psVSD – physical structure vacuolar sorting determinant

PVC – Prevacuolar Compartment

Rpm – rotation per minute

RT – Room Temperature

SDS – Sodium dodecyl sulphate

SDS-PAGE – SDS-Polyacrylamide gel electrophoresis

SNARE - soluble N-ethylmaleimide sensitive factor adaptor protein receptor

SP – Signal Peptide

ssVSD – sequence specific vacuolar sorting domain

TAE – Tris-acetate-EDTA buffer

TBS-T - Tris buffer saline with tween 20

TCA – Trichloroacetic acid

TEMED - N, N, N', N'-Tetramethylethylenediamine

TGN – Trans-Golgi network

TIP – Tonoplast Intrinsic Protein

UV - UltraViolet

V - volt

VSD – vacuolar sorting determinant

VSR – vacuolar sorting receptor

1. INTRODUCTION

The plant cell wall is a compartment with unique characteristics and relevant role in several cellular mechanisms. The synthesis and remodeling of the cell wall unquestionably implies numerous secretion and biosynthesis processes, though the protein trafficking pathways to and from this compartment, as well as its regulation, are yet poorly understood. Recently, new data has emerged regarding the existence of signals and intermediates to control those pathways, questioning the definition of the *default* pathway as a secretion route with no need for control mechanisms. Using the aspartic proteinases cardosin A and cardosin B as experimental models, our aim was to unveil the effects of the presence/absence of cell wall in the regulation of protein sorting, namely in vacuolar trafficking. Hence, the design of an experimental strategy required an overview of the endomembrane system, as well as the protein transport routes among organelles of the secretory and endocytic pathway and the cell wall. Furthermore, a quick survey on the main features of plant aspartic proteinases was needed, particularly on cardosin A and cardosin B, as a way of better understanding the protein models used.

1.1. The Endomembrane System

In contrast to prokaryotes, the eukaryotic cell is divided into compartments enclosed by membranes, allowing cells to specialise given that each compartment performs a different function. The functionality of this compartmentalisation relies on an efficient and well-organised exchange of cargo molecules between compartments, from synthesis to final destination. Hence, the endomembrane system is a key feature of eukaryotic cells, maintaining and controlling the trafficking of macromolecules as well as preserving the inner properties of intracellular organelles (Foresti & Denecke 2008; Carter et al. 2004). The endomembrane system consists of a set of specialised organelles, morphologically and functionally unique, which have important roles in the production and modification of macromolecules within the cell, as well as in their transport. The system comprises organelles from the secretory and endocytic pathways, including the endoplasmic reticulum (ER), the Golgi apparatus (GA), the trans-Golgi network (TGN), pre-vacuolar compartments (PVC), lytic and protein storage vacuoles (LV/PSV), the endosomes and the plasma membrane (Nebenführ 2002). As the secretory pathway manages the transport of newly formed molecules from the ER to their final destinations such as vacuoles or plasma membrane, the endocytic route leads molecules which have entered the cell for degradation/recycling. The system works as a whole, as a way of maintaining a dynamic equilibrium and functional integrity, upon which the life of the cell depends on (Satiat-Jeunemaitre et al. 1999; Hanton et al. 2005).

Apparently, the same machinery is used by plants and other systems, such as mammals or yeast, for the handling of macromolecules through the secretory pathway. Nevertheless, despite the identification of plant homologs for several transport-related proteins in other systems, plants seem to have evolved unique characteristics in order to optimise protein transport. For instance, the presence of protein storage vacuoles and a close connection between the endomembrane system and the cytoskeleton in plant cells represents a contrast with their mammalian and yeast counterparts. Furthermore, the ER of plant cells is pushed to the periphery by the large central vacuole contrastingly to the mammalian ER; however, its export sites (ERES) are highly motile despite the space constraint, whereas in mammals the ER is hardly motile. The absence of an intermediate organelle between the ER and the Golgi apparatus, the high motility and dynamics of the Golgi and the complexity and variety of cargo transport pathways, are also key features that distinguish the plant endomembrane system from similar ones (Hanton et al. 2006; Hanton et al. 2005; Nebenführ 2002).

1.1.1. The Endoplasmic Reticulum

The endoplasmic reticulum stands as the entry point into the secretory pathway. Mainly from the cytosol, newly synthesised soluble proteins enter the ER cotranslationally, led by an N-terminal signal peptide, which is subsequently cleaved by a luminal signal peptidase while the new polypeptide emerges into the ER lumen. Membrane proteins may also have a signal peptide or, in other cases, inner protein domains which regulate ER entrance. The translocation into the ER involves multiprotein aqueous pores, the translocon pores, through which the nascent polypeptide moves before emerging into the ER lumen. The polypeptide translocation across the ER membrane, the only membrane that needs to be crossed along the pathway, requires no energy. The folding of the newly synthesised polypeptide starts in the ER lumen, assisted by protein folding helpers, such as the BiP chaperone, calreticulin and protein disulfide isomerase (PDI). The N-glycosylation of many secretory proteins also occurs in the ER lumen, at the luminal side of the translocon pores (Vitale & Denecke 1999). If the conformational maturation cannot be successfully accomplished, the proteins are targeted for degradation in a process commonly known as “quality control” and dislocated in most cases to the cytosol for further disposal (Vitale & Ceriotti 2004).

1.1.2. The ER – Golgi Interface

Protein transport between the ER and the Golgi apparatus is thought to be mediated mainly by coated protein complex (COP) vesicles, controlled by small GTPases (Fig 1). Export from the ERES to the Golgi requires the recruitment of COPII vesicles, which have the role of transporting newly synthesised proteins. The anterograde transport of molecules from ER to Golgi must be balanced with a backwards recycling transport. Hence, the retrograde transport, mediated by COPI vesicles, intents to retrieve from the Golgi specific molecules such as proteins that escape to the Golgi but are supposed to be resident within the ER, membrane lipids, or proteins that are actually involved in the anterograde transport but can be reclaimed back to the ER for further reuse (Hanton et al. 2005; Vitale & Ceriotti 2004).

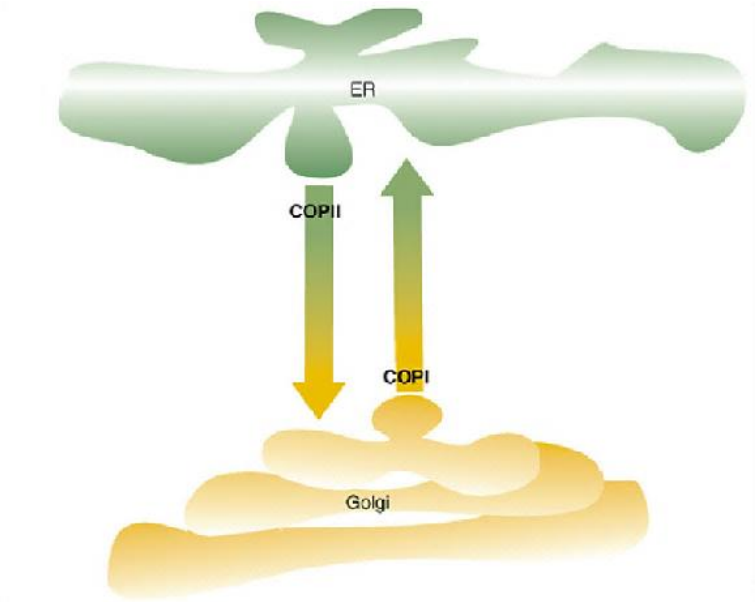

Figure 1 - Schematic representation of the cargo transport between the ER export sites and the Golgi apparatus. The transport from ERES to Golgi – anterograde transport – is mediated by COPII vesicles, while the backwards recycling transport – retrograde transport – is mediated by COPI vesicles. Adapted from Matheson et al. 2006.

The mechanisms behind the regulation of the COP vesicles recruitment are yet poorly understood. Is has been accepted that soluble proteins exit the ER via a bulk-flow mechanism, according to which the vesicle budding is spontaneous and constant, thus the retrograde transport becomes vital when it comes to retrieving ER resident proteins (Vitale & Denecke 1999). However, the existence of receptors on the vesicles' membrane cannot be excluded and an active transport model for anterograde transport is still a valid possibility (Matheson et al. 2006). The retrograde transport of soluble proteins, on the other hand, has been shown to be controlled by specific signals, such

as the carboxy-terminal H/KDEL motif. The latter interacts with the cis-Golgi, triggering the formation of COPI vesicles and the retrieval of ER resident proteins (Hanton et al. 2006).

The early plant secretory pathway has shown to be highly dynamic and so, the motility of the ER and Golgi stacks has originated a series of hypothesis trying to explain how exactly the protein transport occurs between the two organelles. The first hypothesis to be postulated was the “vacuum cleaner” model, according to which ERES are randomly distributed along the surface of the ER and the Golgi stacks sweep over the ER membrane, constantly capturing export vesicles (Fig 2, A). The stop-and-go model, on the other hand, proposes the existence of fixed ERES on the ER membrane and thus, by a yet unknown signal by ERES, the Golgi bodies would become temporarily detached from the actin filaments and halt their movement while the vesicles are transferred (Fig 2, B). More recently, a third model was hypothesised, the “mobile ERES”, where the cargo transport occurs in a continuous manner. The ERES and the Golgi stacks would be closely linked and therefore move together, although the nature of this connection is not yet widely understood (Fig 2, C) (Hanton et al. 2005; Hanton et al. 2006). Furthermore, the ER-Golgi cargo transport is known not to require energy nor the intervention of the cytoskeleton (Brandizzi & Snapp 2002).

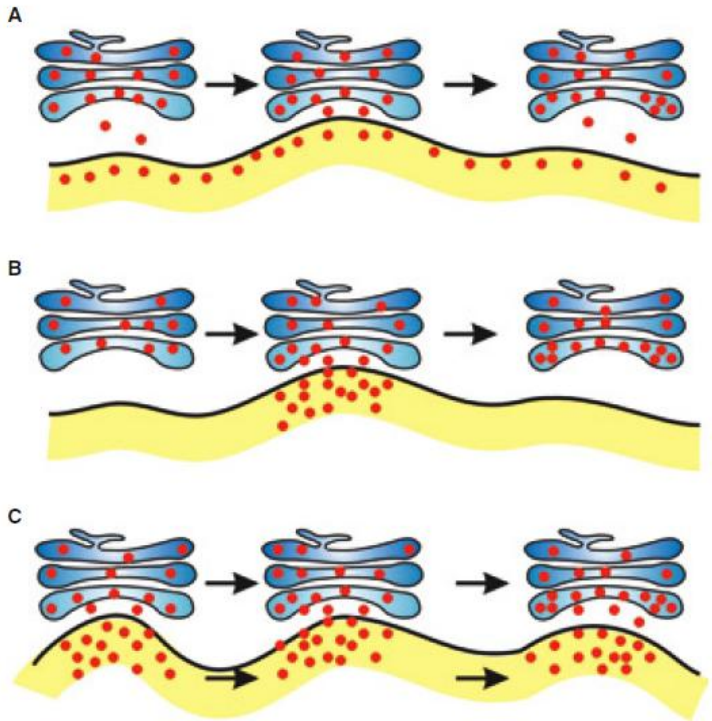

Figure 2 - Schematic models of ER-Golgi protein transport. **A –** “Vacuum cleaner” model. **B –** “Stop-and-go” model. **C –** “Mobile ERES” model. Adapted from Hanton et al. 2005.

1.1.3. The Golgi apparatus

The Golgi apparatus holds a pivotal position among the organelles of the endomembrane system, for its importance in the assembly, processing and sorting of proteins going through the secretory pathway. It is involved in the synthesis of glycoproteins, glycolipids as well as cell wall matrix polysaccharides. The Golgi is commonly described as a tubulo-saccular structure with cisternal morphology, divided into individual and functionally independent stacks, which are able to travel through the cytoplasm along actin filaments. Due to the functional division into cis-face, medium-face and trans-face, each stack is considered a polarised structure, where the cis- generally corresponds to the entry face and the trans- to the maturing/exit face. Moreover, the Golgi enzymes follow a gradient distribution along the stack, changing activity gradually from cis- to trans-face to cope with metabolic events in a progressive manner (Hawes & Satiat-Jeunemaitre 2005; Nebenführ & Staehelin 2001).

The Trans-Golgi Network (TGN) is associated with the trans-face of Golgi stacks. The exact nature of this structure in plants is still a blur and controversy is yet a constant regarding its actual existence in plant cells. Despite the debate, the TGN seems to play a role in the packaging and targeting of cargo molecules leaving the Golgi apparatus, possibly working as an early-endosome (Kang et al. 2011; Park & Jürgens 2011).

1.1.4. Post-GA transport

The Golgi apparatus operates as a sorting station for cargo molecules travelling through the endomembrane system, from which trafficking routes diverge into different directions, including the vacuoles or the plasma membrane. The sorting of cargo molecules throughout the trafficking routes is dependent on carrier vesicles and the prevention of vesicle mislocalisation requires the recruitment of several proteins and factors, such as small GTPases and SNARE (soluble N-ethylmaleimide sensitive factor adaptor protein receptor) complexes (Jurgens 2004; Cai et al. 2007). A number of post-Golgi organelles have been identified as intermediate stations, comprising the trans-golgi network/early endosome, pre-vacuolar compartment/multivesicular body/late endosome, two types of vacuoles and the cell plate, even though the latter is a temporary organelle (Tse et al. 2004; Richter et al. 2009).

Protein Trafficking to the Vacuoles

Vacuoles are true hallmarks of the plant cell, valuable in terms of versatility and functional diversity. The vacuoles are involved in several processes within the cell, such as protein degradation, maintenance of turgor pressure, accumulation of ions and secondary metabolites, programmed cell death and intracellular digestion of disposable components. Currently, two types of vacuoles are known to exist: the lytic vacuole (LV) and the protein storage vacuole (PSV). The latter is usually found in seeds or protein storage specific tissues for its ability to accumulate reserve material, while the LV is common in vegetative tissues. Due to its acidic and hydrolytic nature, the LV has a role in protein degradation and is frequently compared to the animal lysosome (Marty 1999). The outer membrane of each type of vacuole, named the tonoplast, is characterised by the presence of specific aquaporins, the Tonoplast Intrinsic Proteins (TIP). Thus, the presence of α-TIP indicates a protein storage vacuole, whereas the presence of γ-TIP indicates a lytic vacuole (Martinoia et al. 2007). It was recently shown that the two types of vacuoles may co-exist in the same cell. In mature cells, the LV and the PSV presumably merge when an isolated PSV is no longer needed, originating a large unique vacuole (Vitale & Raikhel 1999). The presence of the two types of vacuole in the same cell implies the existence of distinct sorting mechanisms to allow protein trafficking to each vacuole (Paris et al. 1996). Protein sorting to the vacuoles relies on specific vacuolar sorting determinants (VSD), which usually consist of N-terminal sequence specific VSD (ssVSD) or C-terminal VSD (ctVSD) cleavable signals. The ssVSD are known to be involved in the sorting to the lytic vacuole, whereas the ctVSD are generally found to lead proteins to the PSV. A third group of VSD is the physical structure VSD (psVSD), which comprises an internal region of the protein that is often cleaved during protein maturation. The psVSD are commonly found in storage proteins (Neuhaus & Rogers 1998).

The ssVSD is typically an NPIR motif or similar, which is recognised in the Golgi by BP80, a Golgi resident vacuolar sorting receptor (VSR). The BP80 receptor is involved in the recruitment of clathrin coated vesicles (CCV), in which the cargo molecules are transported from the Golgi to the PVC/MVB. The receptor is released from the cargo as soon as the vesicles reach the outer membrane of the PVC/MVB and is promptly recycled back to the Golgi apparatus. The delivery of the cargo proteins to the lytic vacuole is presumably accomplished by fusion of the PVC/MVB with the tonoplast (Richter et al. 2009).

When in route to the PSV, proteins are accumulated into dense vesicles (DV) in the Golgi apparatus. From the Golgi, DVs deliver their cargo directly into the PSV, fusing their membrane with the tonoplast. However, recent evidence suggests that CCV might also be involved in the sorting of storage proteins to the PSV, after interaction with BP80 receptor in

the Golgi apparatus (Hawes & Satiat-Jeunemaitre 2005). Another theory is that storage proteins might be transported to the PSV by means of precursor-accumulating vesicles (PAC), which can accumulate cargo directly from the ER or glycosylated cargo from the Golgi apparatus. Similarly to CCVs, PAC vesicles deliver their cargo by direct fusion with the PSV tonoplast. Moreover, it is currently uncertain if any post-Golgi compartment is involved in the sorting to the PSV, as the PVC/MVB or a similar compartment are suggested as hypothesis (Fig 3) (Jolliffe et al. 2005).

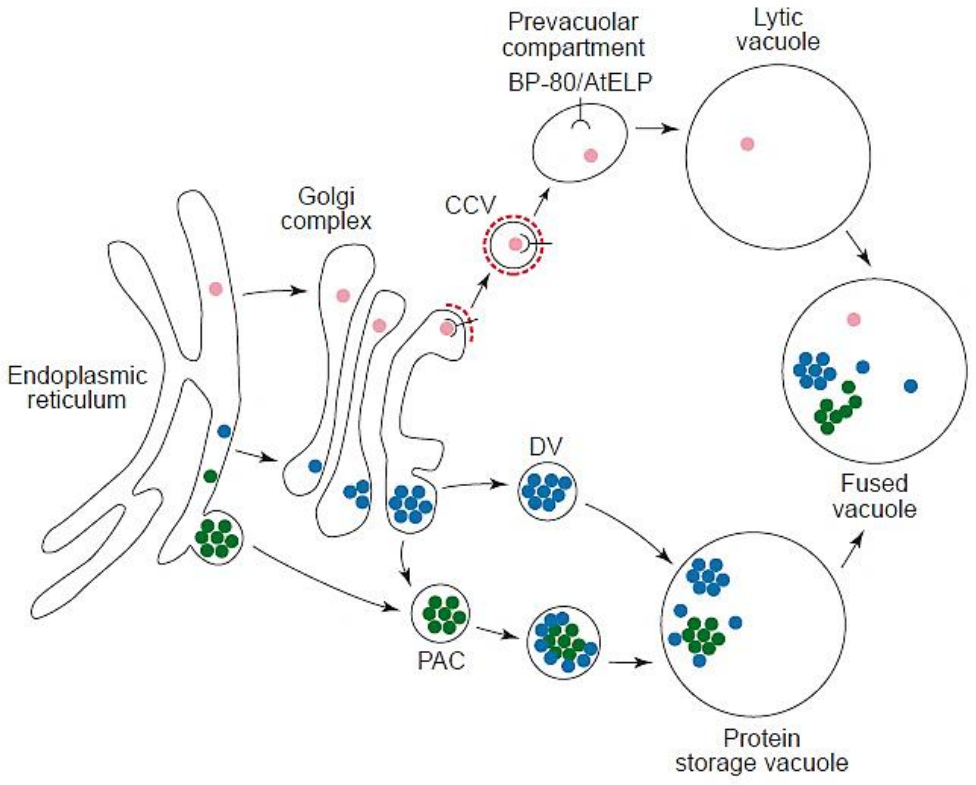

Figure 3 - Schematic representation of soluble proteins transport to the vacuoles. The route to the lytic vacuole is represented by the pink dots. The soluble proteins in route to the lytic vacuole hold an ssVSD, which is recognised by the BP80 vacuolar sorting receptor in the Golgi apparatus. The BP80 receptor is involved in the recruitment of clathrin coated vesicles (CCV; clathrin coat is represented by the broken red line), which transport the cargo proteins to the prevacuolar compartment. The cargo is delivered to the lytic vacuole by fusion of the vesicles with the tonoplast, while the receptor is recycled back to the Golgi apparatus. Proteins in route to the protein storage vacuole hold a ctVSD and might be transported through different pathways, comprising the recruitment of dense vesicles (DV) at the Golgi apparatus, which deliver the protein cargo directly into the PSV, or the recruitment of precursor-accumulating vesicles (PAC), which can accumulate cargo directly from the ER to the PSV or glycosylated cargo from the Golgi to the PSV. In certain conditions, the lytic and protein storage vacuoles might merge, originating a large and unique vacuole (fused vacuole) which performs both lytic and protein storage functions. Adapted from Vitale & Raikhel 1999.

Protein Trafficking to the Cell Wall

The plant cell wall is a unique and dynamic structure with a vital role in cell division and growth, shape maintenance, cell defence and signalling (Szymanski & Cosgrove 2009). The architecture and biogenesis of this structure involves complex processes of biosynthesis and secretion; hence, the structural integrity of the cell wall and consequently the integrity of the plant cell count on the perfect regulation and synchronisation of these processes. Vesicular flow is mainly directed towards the cell wall, due to the need of transporting structural proteins and polysaccharides from the Golgi apparatus, such as wall-modifying enzymes, cellulose synthesis enzymatic complexes, pectins and hemicelluloses. Although the endomembrane system and the cell wall are intrinsically connected, the trafficking pathways of proteins to and from the plant cell wall are yet poorly understood (Rose & Lee 2010; De Caroli et al. 2011; Wightman & Turner 2010). The sorting of soluble proteins to the cell wall has been thought to follow a *default* route. Apart from the signal peptide needed for ER entrance, no signals or receptors were found to be involved in the regulation of this pathway and currently little is known regarding the intracellular route followed by the secretory vesicles before reaching the PM-CW complex (Denecke et al. 1990; Foresti & Denecke 2008; Rojo & Denecke 2008). In the last few years, the mechanisms that regulate the sorting to the cell wall as well as the routes taken by the cargo vesicles have become an important matter of discussion, as new data and plausible intermediates have been identified. Nonconventional routes to the cell surface have also been identified in eukaryotes, where proteins holding a signal peptide for entering the secretory pathway reach the plasma membrane by a COPII independent manner, presumably bypassing the Golgi (Nickel & Seedorf 2008; Nickel & Rabouille 2009). Routes for protein trafficking to the extracellular matrix involving the endosome have also been proposed. Plant endocytosis is a recently accepted process and so, endocytic compartments are yet to be thoroughly characterised (Müller et al. 2007). Nonetheless, a straight connection between the secretory and endocytic pathway has been suggested. Additionally, the two pathways would have organelles in common, where the routes would converge. The endocytosis process consists on the vesicle mediated uptake of cargo molecules from the extracellular matrix through the plasma membrane. The internalisation of the vesicles is followed by the transport of the cargo to endosomal compartments. The molecules are first delivered to the late endosome, presumably the PVC/MVB, from where they are either directed to a recycling pathway or to the lytic vacuole for degradation. The endocytic pathway, as well as its association with the secretory pathway, is still a matter of debate among the scientific community and many question marks are yet to be solved (Robinson et al. 2008; Samaj et al. 2005).

1.2. Cardosins – Models for Protein Sorting Studies

Cardosins – Aspartic Proteinases

Cardosins are plant aspartic proteinases (AP) that were first isolated from the flowers of cardoon (*Cynara cardunculus* L.). Cardoon is quite an important plant in Portugal and Spain, where it is mainly distributed, due to the use of the milk clotting activity of APs to manufacture several types of cheese (Cordeiro et al. 1994). Although six more have been posteriorly identified, the first cardosins to be isolated – A and B – are beyond a doubt the better characterised, from molecular to biosynthesis and compartmentalisation levels (Veríssimo et al. 1996; Ramalho-Santos et al. 1998; Vieira et al. 2001; Pissarra et al. 2007). Despite all the research that has been developed during the past decade, the biological roles of these proteins are still unknown. Nonetheless, putative roles have been suggested, such as in the germination and development of seeds, storage protein conversion, flower senescence, defensive mechanisms and reproduction (Figueiredo et al. 2006; Pissarra et al. 2007; Pereira et al. 2008). Similarly to most APs, cardosins A and B are synthesised as preproenzymes, holding an N-terminal signal peptide, on which they rely for entering the secretory pathway through the ER, followed by a conserved pro-segment which is supposed to be involved in protein interaction with the active site (Kervinen et al. 1999). Apart from the signal peptide and the pro-segment, cardosins are divided into N-terminal and C-terminal domains, separated by a region of about 100 aminoacids – the *Plant Specific Insert* (PSI) domain (Ramalho-Santos et al. 1997). The PSI is a saposin-like domain, common to the most part of plant APs, which is thought to be involved in the proper folding and stability of the proteins, to interfere with the permeability of cell membranes and to be part of defence and signalling mechanisms (Mazorra-Manzano et al. 2010). During protein maturation along the secretory pathway, cardosins are processed through a series of events that lead to successive cleavages of the regions comprising the precursor (Fig 4). For cardosin A, the first step is the separation of the N-terminal domain from the PSI domain, followed by a total separation of the PSI. The pro-segment is the last region to be cleaved. For cardosin B, the process has not been thoroughly clarified, though its processing is thought to occur in the same way as for cardosin A (Ramalho-Santos et al. 1998; Vieira et al. 2001).

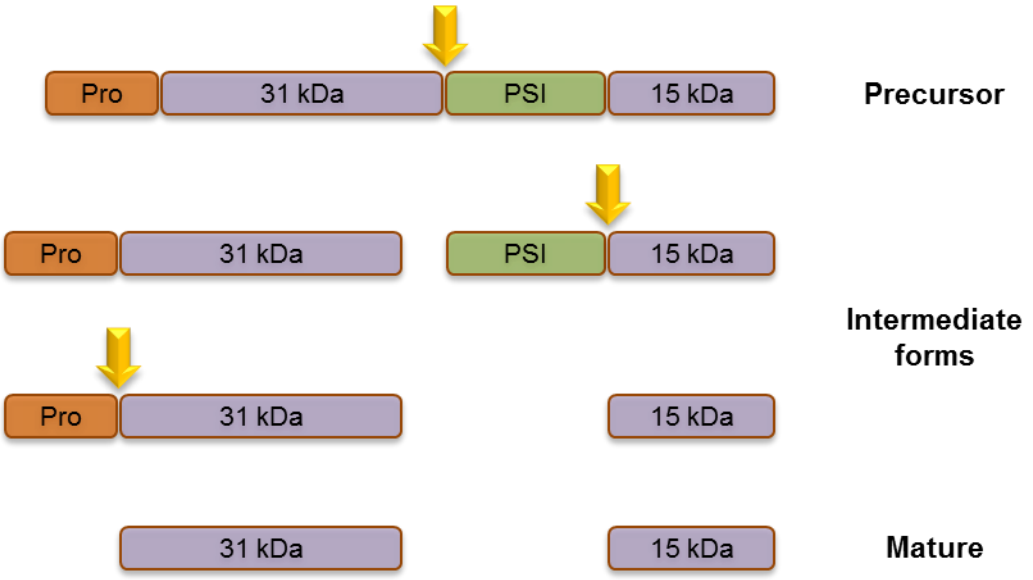

Figure 4 - Schematic representation of the proposed sequence of events during the processing of cardosin A. The first cleavage separates the N-terminal region from the PSI domain, followed by the complete excision of the PSI and finally the Pro-segment is removed, originating the mature form.

Cardosins and Protein Sorting

Despite their high similarity, cardosins A and B are directed to different locations in the floral tissues of *C. cardunculus*. While cardosin A is an intracellular protein, mainly found in the vacuoles of the stigmatic papillae, cardosin B is found in the extracellular matrix of both stigma and style transmitting tissue (Duarte et al. 2008; Ramalho-Santos et al. 1997; Vieira et al. 2001). As cardoon is difficult to transform, heterologous systems such as *Nicotiana tabacum* or *Arabidopsis thaliana* are commonly used for trafficking studies in cardosins. The localisation pattern of these proteins is slightly modified when transiently expressed in leaf epidermis cells of *N. tabacum*, as both cardosins were observed accumulating in the lytic vacuole (Duarte et al. 2008; da Costa et al. 2010). Curiously, in *N. tabacum* mesophyll protoplasts expressing cardosin B, secretion assays performed in our group have shown secretion of the protein. So, the presence/absence of the cell wall might have an influence on the regulation of the sorting of cardosins (da Costa et al. 2010).

Recently in our group, two vacuolar sorting determinants were identified among the domains of cardosins A and B – the C-terminal peptide and the PSI domain. The C-terminal of cardosins was shown to efficiently target the protein to the lytic vacuole when placed at the C-terminus of the fusion protein. Moreover, similarly to the observed for other APs' C-terminal peptides, it showed to be sufficient for the correct sorting of the proteins to the vacuole (Pereira et al. 2012, submitted). The C-terminal mediated transport has shown to follow a COPII dependent route from the ER to the Golgi apparatus, transporting the protein

through the classical pathway leading to the vacuole. Unlike the C-terminal, the PSI domain in not a common VSD among APs, although it has shown to successfully direct cardosins A and B to the vacuole. However, the PSIs from cardosin A and B direct the protein to the vacuole using different intracellular routes. While the PSI from cardosin B leads the protein to the vacuole through the Golgi apparatus, the PSI from cardosin A seems to bypass the Golgi, in a COPII independent manner (Pereira et al. 2012, submitted). Moreover, the association of the PSI with biological membranes has been demonstrated in vitro (Egas et al. 2000) and also in the plasma membrane/cell wall complex in cardoon seeds (Pereira et al. 2008). In the early stages of *C. cardunculus* reproduction, particularly during pollination, cardosin A needs to be transported to the cell wall in order to connect with a pollen receptor (Faro et al. 1999), an association presumably mediated by the PSI domain. Therefore, the involvement of a VSD, particularly the PSI domain, in the regulation of cardosins' sorting in the presence or in absence of the cell wall is definitely a hypothesis worth exploring.

1.3. Objectives of the Thesis

The protein transport routes to and from the plant cell wall have been drawing more and more attention from the scientific community, as they are essential for the integrity of this structure and consequently for the functional maintenance of the plant cell. Evidence has emerged indicating that the cell wall, as one of the main components of the cell and an interface between the cell and the outside environment, could in fact be involved in the regulation of protein transport events. Recent results in our lab, using *N. tabacum* mesophyll protoplasts and cardosins B as experimental model, have indicated that the presence/absence of the cell wall might influence the destination of this protein. Hence, the main objective of this thesis was to **unveil if the cell wall actually regulates protein sorting, using cardosins A and B as experimental models and *N. tabacum* mesophyll protoplast during cell wall regeneration**. Mesophyll protoplasts isolated from *N. tabacum* leaves transformed with chimeric constructions of cardosin A and cardosin B fused to mCherry were used in secretion assays for the study of the cell wall regulation on the sorting of cardosins. The analysis was performed through confocal microscopy and biochemical analysis during cell wall regeneration.

Cardosin A and cardosin B are both destined for the vacuole in *N. tabacum* leaf, directed by two identified VSDs – the C-terminal region and the PSI domain. To pursue a **possible connection between the identified VSDs and the sorting of cardosins in absence of the cell wall and during its regeneration** was also an objective of this thesis. Chimeric constructions of the C-terminals and PSIs from cardosins A and B fused to mCherry were used for the transformation of *N. tabacum* leaves, for further protoplast isolation and secretion assays were performed in a similar way as for cardosins A and B. As protoplasts from *N. tabacum* during cell wall regeneration were used throughout the assays, **an optimisation of protoplast culture and cell wall regeneration conditions are essential for the planning of the secretion assays**.

Evidences have shown that the PSI from cardosin A is prone to interact with biological membranes, as it was shown in vitro as well as in cardoon seeds. It was also demonstrated that PSI A follows an intracellular route to the vacuole which is different from the usually followed by C-terminal peptides, bypassing the Golgi in a COPII independent manner. Hence, it is also our aim to better **understand the maturation process of cardosin A and the role of the PSI domain in the sorting of this protein.** A site directed-mutagenesis approach was chosen for this task, so as to impair the cleavage of the PSI domain during protein maturation and further analyse the eventual changes in protein processing and sorting. The planning of this experimental strategy was done in collaboration with the Theoretical Chemistry Group of the Faculty of Chemistry in Porto University.

2. METHODOLOGY

2.1. Dissecting the role of the plant cell wall in the regulation of protein trafficking

2.1.1. Germination and maintenance of *Nicotiana tabacum* SRI cv. Petit Havana

N. tabacum seeds were allowed to germinate in Petri dishes on top of moistened filter paper. After 10-15 days at 22 ºC with 16 hours photoperiod, the seedlings were transferred individually to plant substrate (SIROPlant) and kept under the same conditions.

2.1.2. Isolation of protoplasts from *Nicotiana tabacum* leaves

Half of an infiltrated *N. tabacum* leaf was used for the isolation of protoplasts. The leaf was cut into small pieces and the lower epidermis was carefully removed with a tweezer. The small pieces of leaf were placed in Petri dishes with the lower epidermis facing down, floating in 8 mL of TEX medium [3 mM NH_4NO_3, 5 mM $CaCl_2.2H_2O$, 2.4 mM MES and 0.4 M sucrose, in B5 Gamborg medium (Duchefa)] containing 1% (w/v) cellulase and 0.25% (w/v) macerozyme, and incubated overnight in the dark, at room temperature. Subsequently to the digestion, the protoplasts were gently released from the leaf portions with a plastic pipette and recovered into a new Petri dish through a 100 µm nylon mesh, prior to being transferred to 15 mL centrifuge tubes. The protoplasts suspension was then overlaid with 1 mL of 0.4 M mannitol/W5 medium [W5 solution: 154 mM NaCl, 125 mM $CaCl_2$, 5 mM KCl, 5 mM glucose and 1.4 mM MES, pH 5.6, filter sterilised (0.4 M mannitol/W5 solution, in a proportion of 4:1)] and centrifuged at 100 x g, acc/des 1, for 10 minutes. The living protoplasts, floating beneath the mannitol/W5 layer, were promptly recovered into a new 15 mL centrifuge tube containing mannitol/W5 (2/3 of the final volume, allowing the protoplasts to sink) and the two phases were gently mixed together. After a 5 minute centrifugation at 100 x g, acc/des 1, the supernatant was eliminated and the protoplasts stored at low temperature for further use.

2.1.3. Cell wall regeneration in *Nicotiana tabacum* protoplasts

The regeneration of the cell wall in *N. tabacum* leaves is a subject already described in the literature. However, the process of regeneration depends on numerous factors, such as temperature, light, pH, agitation, culture medium and even the health of the actual plants, among others. Thus, optimisation of culture conditions was required, in order to assure cell

viability along the following assays, as well as to define the duration of the assays and the time points for sample collecting.

For optimization purposes, protoplasts of non-transformed *N. tabacum* leaves were isolated as previously described and placed on different culture media [medium A (3 mM NH_4NO_3, 5 mM $CaCl_2.2H_2O$, 2.4 mM MES and 0.4 M sucrose, in B5 Gamborg medium (Duchefa)) or medium B (0.7 M D-mannitol, 0.2 mM KH_2PO_4, 1 mM KNO_3, 1 mM $MgSO_4$, 10 mM $CaCl_2$, 1 µM KI, 0.01 µM $CuSO_4$, 1 µg/mL thiamine HCl, 100 µg/mL myo-inositol and 2 µg/mL glycine, pH 5.8, filter sterilized)]. Other factors were tested, such as the temperature, the presence/absence of light and the presence/absence of agitation. The viability of the cells was monitored by optical microscopy and the regeneration of the cell wall was observed over time by fluorescence microscopy, by means of a fluorescent stain – Calcofluor White ST (0.01%) – which strongly binds to cellulose, allowing the observation of *de novo* formation of cell wall, coloured white under UV light.

2.1.4. Infiltration of *Nicotiana tabacum* leaves

A. tumefaciens transformed cultures were inoculated into LB medium with the appropriate antibiotic and grown overnight at 28 ºC with 200 rpm orbital shaking. From the overnight culture, 1 mL was transferred to a 1.5 mL tube and centrifuged at 14000 x g for 1 minute. The cells were then resuspended in 1 mL of infiltration buffer (10 mM $MgCl_2$, 10 mM MES, pH 5.6, filter sterilised) and centrifuged twice more, being however resuspended in infiltration buffer supplemented with 100 µM acetosyringone (4′-Hydroxy-3′,5′-dimethoxyacetophenone 97%, Sigma-Aldrich), in order to increase the virulence of the *Agrobacterium*. Absorbance measurements at 600 nm with 1/5 dilutions of cell suspensions preceded the infiltration. For each clone, an infiltration mixture was prepared with cell suspension and infiltration buffer with 100 mM acetosyringone, according to the following equation [($OD_{desired}/OD_{observed}$).1000/5], where the desired OD was 0.1-0.3. The infiltration was performed in *N. tabacum* leaves, using a 1 mL plastic syringe (without needle) and placing the tip against the abaxial surface. The plunger was pressed gently, while supporting the adaxial surface with the finger, causing the suspension to diffuse through the leaf and into the mesophyllar air spaces. The plants were incubated at the same light/temperature conditions as previously described for germination and maintenance.

2.1.5. Secretion assays

N. tabacum leaves were infiltrated with different cardosin A and cardosin B constructions fused to the fluorescent protein mCherry. The constructions used were already available in the laboratory and inserted into pVKH18En6 binary vector, ideal for transient expression in *N. tabacum* leaves.

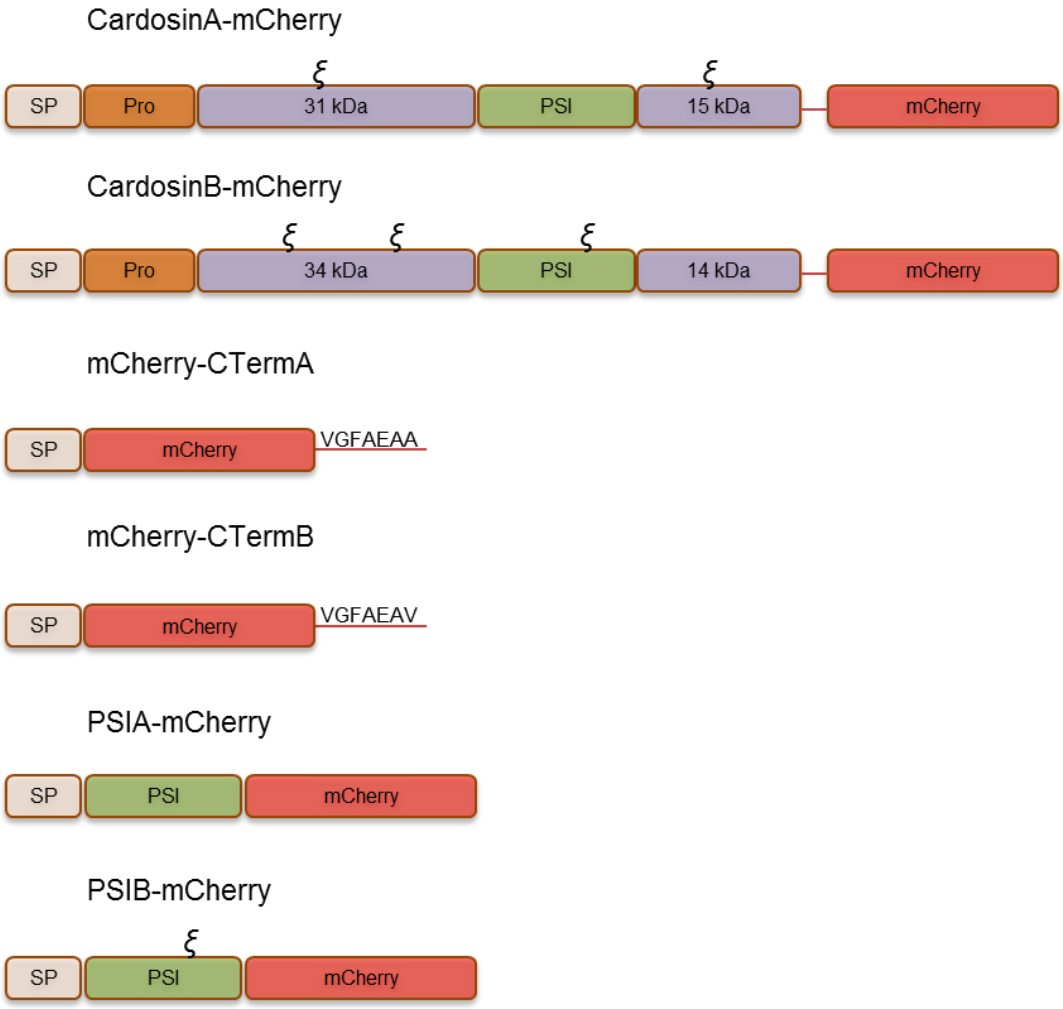

Figure 5 - Schematic representation of the chimeric constructions used in this study. Constructions coding for cardosin A and B, the PSI from cardosin A and B, and the C-terminal from cardosin A and B, fused to the fluorescent protein mCherry. The ξ symbol represents the glycosylation sites.

Approximately 24 hours after infiltration, to allow the transgene expression, protoplasts were isolated and incubated in 6 mL of medium B, in the dark at 22 ºC. At different time-points (0, 4, 8, 24, 30 hours), 1 mL samples were taken, separating the cells from the culture medium by letting the protoplasts afloat or sink, depending on the culture medium used. Different protein extraction treatments were applied to cells and culture medium fractions. Subsequently to the protein extractions, the samples were analysed by

Western Blotting. At the same sampling time-points, protoplasts and leaves were analysed under Confocal Laser Scanning Microscopy.

2.1.6. Protein extraction from protoplasts

To each sample of cells from the secretion assay, 75 µL of extraction buffer [50 mM sodium citrate pH 5.5, 5% (w/v) SDS, 0.01% (w/v) BSA, 150 mM NaCl, 2% (v/v) β-mercaptoethanol and 10 µL "Protease Inhibitor Cocktail" (Sigma) per 300 mg of fresh tissue] were added. Once mixed with the buffer, the samples were boiled for 10 minutes, prior to a 30 minute centrifugation at 14000 x g. The supernatant was then recovered to a new tube, and proteins quantified on Qubit™ Fluorometer (Invitrogen) according to the manufacturer's instructions and stored at -80 ºC.

2.1.7. Preparation of proteins from protoplasts' culture medium by Trichloroacetic acid (TCA) precipitation

To each culture medium sample from the secretion assay, one volume of 20% (w/v) TCA was added. After vortex homogenisation, the samples were incubated on ice for 15 minutes, preceding a 15 minute centrifugation at 14000 x g, in a refrigerated centrifuge (6 ºC). The resulting supernatant was discarded and 1 mL of ice-cold acetone was added, without resuspending the pellet, followed by another 15 minute centrifugation, similar to the previous one. The sediment was once more washed with acetone and air-dried at room temperature. Afterwards, the samples were resuspended in 75 µL of extraction buffer (same buffer as in 3.2.6), boiled for 5 minutes and centrifuged briefly at 14000 x g. The supernatant was then recovered to a new tube, and proteins quantified on Qubit™ Fluorometer (Invitrogen) and stored at -80 ºC.

2.1.8. SDS-PAGE and Western blotting

The SDS-PAGE (sodium dodecyl sulphate polyacrylamide gel electrophoresis) is widely used for the separation of proteins according to their electrophoretic mobility, which diverges depending on the length of the polypeptide chain, protein folding and post-translational modifications. Samples containing approximately 15 µg of total protein were prepared with a 1:5 dilution of loading buffer [0,225 M Tris-HCl pH 8, 50% (v/v) Glycerol, 5% (w/v) SDS, 0.05% (w/v*)* Bromophenol blue and 0.25 M DTT] and by incubation at 65 ºC for 5 minutes. The proteins were then loaded in the gel electrophoresis system (Cleaver Scientific), with a 4% stacking gel [2,1 mL ddH_2O, 495 µL acrylamide (30% Acrylamide/Bis Solution, BioRad),

375 µL 0.5 M Tris-HCl pH 6.8, 1.5 µL phenol red, 30 µL 10% (w/v) SDS, 30 µL 10% (w/v) APS (ammonium persulfate, Sigma) and 10 µL TEMED (N,N,N′,N′-Tetramethylethylenediamine, Sigma)] and a 12.5% resolving gel [3.14 mL ddH_2O, 4.16 mL acrylamide (30% Acrylamide/Bis Solution, BioRad), 2.5 mL 1,5 M Tris-HCl pH 8.8, 100 µL 10% (w/v) SDS, 100 µL 10% (w/v) APS (ammonium persulfate, Sigma) and 10 µL TEMED (N,N,N′,N′-Tetramethylethylenediamine, Sigma)]. The molecular weight marker used was PageRuler Plus Prestained Protein Ladder (Thermo Scientific). Samples were electrophoresed by the application of an electric current of 100 V across the gel. After electrophoresis, the proteins were transferred onto a nitrocellulose membrane (Protran - Nitrocellulose Transfer Membrane, Whatman) for 1 hour at 100 V, using a Tris-glycine-methanol buffer (25 mM Tris, 192 mM Glycine, 20% (v/v) Methanol). Once the transfer was complete, the membrane was incubated in blocking solution [5% (w/v) milk powder (Molico, Nestlé), 1% BSA (Bovine Serum Albumin, Sigma-Aldrich) and 0.5% (v/v) Tween 20 in TBS-T buffer (50 mM Tris, 200 mM NaCl and 0.1% (v/v) Tween 20)] for 1 hour at room temperature, prior to an overnight incubation at 4 ºC with the primary antibody in blocking solution. For cardosin A, a specific antibody raised against the large subunit (CRAHSMYESSD) was used in a dilution of 1:1000. For cardosin B, an antibody raised against its large subunit was used (CVIHPRYDSGD) in a dilution of 1:1000. For C-terminal and PSI fusions with mCherry, an antibody raised against mCherry (Invitrogen) was used in a dilution of 1:1000. For the burst controls of secretion assays, an antibody raised against calreticulin was used in a dilution of 1:2000 (Denecke et al. 1995). The membrane was then washed three times (10min, 5min, 5min) with TBS-T and incubated with the secondary antibody [1:1000 dilution of anti-rabbit IgG conjugated to Alkaline Phosphatase (Vector)] for 30 minutes, at room temperature. The membranes were washed three times (10min, 5min, 5min) with TBT-T once more and the detection was performed using a chromogenic substrate for Alkaline Phosphatase (NBT/BCIP, Promega).

2.1.9. Fluorescence Microscopy and Confocal Laser Scanning Microscopy

For the monitoring of cell wall regeneration during time points optimization, protoplasts were observed through fluorescence microscopy. Prior to observation, a small portion of cell suspension was placed on a microscope slide and Calcofluor White ST at 0.01% was added. The images were acquired on a fluorescence microscope (Nikon OPTIPHOT-2) using an UV light emission filter.

During the secretion assays, the protoplasts were observed through Confocal Laser Scanning Microscopy. Thus, small portions of cell suspension were placed on microscope

slides for visualisation. On the same time points as the protoplasts' visualisation, the transformed leaves of origin were also observed. Leaf pieces of approximately 1 cm^2 were excised and placed on a glass slide with water, with the abaxial epidermis facing up. The images were acquired on a SP2 Leica Confocal Microscope (Leica Microsystems, Heidelberg) and the excitation wavelength used was 561 nm (for fluorescent protein mCherry).

2.2. Unveiling the role of the PSI domain in the regulation of cardosin A trafficking

2.2.1. Primers design and site-directed mutagenesis

Polymerase Chain Reaction (PCR) was performed in order to originate point mutations in the cleavage sites of the PSI domain of cardosin A and thus, specific primers were designed for both cleavage sites, to block the PSI removal during protein processing (Table 1). During the design of the primers, the possibility of unwanted modifications in the conformation of the protein had to be minimised but, on the other hand, the aminoacidic modifications need to be drastic enough to meet our purpose. So, every mutation was carefully analysed *in silico* by molecular modulation methods. Although the crystallographic structure of the precursor form of cardosin A is not yet available, the modulation can be performed by homology. This work was made in collaboration with the Theoretical Chemistry Group from the Faculty of Sciences.

Table 1 - Primers used for the Site-directed mutagenesis of cardosin A.

Primer	Sequence (5' → 3')	Specifications
AmutPSI_5_fwd	AATCATGCAATTGGCGCTCTCGGGACCAAGCTCCAGCAATGCAAGACAGT	Site mutations (shown in red) at 5' end of the PSI domain
AmutPSI_5_rev	ACTGTCTTGCATTGCTGGAGCTTGGTCCCGAGAGCGCCAATTGCATGATT	Site mutations (shown in red) at 5' end of the PSI domain
AmutPSI_3_fwd	AACGAGTTGTGTGAACACCAAGCCGTTGCAGCTGAAGAATTACAAGTAGA	Site mutations (shown in red) at 3' end of the PSI domain
AmutPSI_3_rev	TCTACTTGTAATTCTTCAGCTGCAACGGCTTGGTGTTCACACAACTCGTT	Site mutations (shown in red) at 3' end of the PSI domain

Two different reactions were performed for the mutation of the cleavage sites, as the 5' site was modified, sequenced and confirmed, prior to the mutation of the 3' one. In the first PCR reaction unmodified cardosin A (inserted in pBluescript II SK plasmid) was used as template while in the second reaction, the confirmed product of the first one was used as template DNA. In both reactions, *Pfu* DNA polymerase (Fermentas) was used, as a way to minimise the incorporation of errors, due to its proofreading activity. The PCR reactions' composition and conditions were as described in tables 2 and 3, respectively.

Table 2 - PCR reactions' composition used for the Site-directed mutagenesis of cardosin A.

Reagent	Final concentration
Sterile distilled water	Up to 25 µL
DNA template	500 ng
Pfu buffer with $MgSO_4$	1x
dNTPs	0,3 mM
Primer Forward	0,4 µM
Primer Reverse	0,4 µM
Pfu DNA polymerase	2,5 U

Table 3 - PCR conditions used for the Site-directed mutagenesis of cardosin A.

Step		Conditions
Initialization		95 ºC – 5 min
16 cycles	**Denaturation**	95 ºC – 30 sec
	Annealing	54 ºC – 30 sec
	Extension	72 ºC – 9 min
Final extension		72 ºC – 15 min

The resulting products of the Site-directed mutagenesis PCR reactions were digested with *DpnI* for 1 hour at 37 ºC followed by inactivation at 65 ºC for 15 minutes, as a way to eliminate the template DNA. Since *DpnI*, a frequent cutter, recognises *Dam* methylated DNA only, all the molecules originated in *E. coli* were degraded. Afterwards, the mutated DNA was used to transform competent *E. coli* and the screening was performed through sequencing (T7 and T3 universal primers; Eurofins MWG Operon), after DNA extraction using GenElute™ Plasmid Miniprep Kit (Sigma-Aldrich), according to the manufacturer's instructions.

2.2.2. Addition of restriction enzyme adaptors

To facilitate the subsequent cloning steps, restriction enzyme recognition sites had to be added to the AmutPSI construction obtained previously, which was accomplished through PCR reactions. Different combinations of restriction enzyme adaptors were used, in order to create AmutPSI_STP (with the stop codon at the end of the sequence) and AmutPSI_noSTP (without the stop codon at the end of the sequence) (Table 4). The construction AmutPSI_noSTP, when cloned into pVKH18-En6 vector, becomes in frame with mCherry, a fluorescent protein encoded by part of this vector, allowing further analysis through CLSM.

Table 4 - Primers used for the addition of restriction enzyme adaptors to AmutPSI construction.

Primer	Sequence (5' → 3')	Specifications
cardA 5' xba	TCTAGAGCCGCCACCATGGGTACCTCAATCAAA	*XbaI* recognition site (in red) added to 5' end of AmutPSI_STP and AmutPSI_noSTP
ARnSTP_sal	GTCGACGCTGCTTCTGCAAATCCAAC	*SalI* recognition site (in red) added to 3' end of AmutPSI_noSTP
R1515_sac	CTGAGCTCTCAAGCTGCTTCTGCAAAT	SacI recognition site (in red) added to 3' end of AmutPSI_STP

In these PCR reactions, Pfu DNA polymerase was used as previously described. AmutPSI was used as template DNA and the components and conditions were as follows in tables 5 and 6, respectively.

Table 5 - PCR reactions' composition used for the addition of restriction enzyme adaptors to AmutPSI construction.

Reagent	Final concentration
Sterile distilled water	Up to 25 µL
DNA template	20-100 ng
Pfu buffer with $MgSO_4$	1x
dNTPs	0,2 mM
Primer Forward	0,3 µM
Primer Reverse	0,3 µM
Pfu DNA polymerase	0,6 U

Table 6 - PCR conditions used for the addition of restriction enzyme adaptors to AmutPSI construction.

Step		Conditions
Initialization		95 ºC – 5 min
30 cycles	Denaturation	95 ºC – 30 sec
	Annealing	54 ºC – 30 sec
	Extension	72 ºC – 3 min
Final extension		72 ºC – 8 min

The products obtained were subjected to horizontal gel electrophoresis, in a 0.8-1% agarose gel prepared in 1x TAE buffer (40 mM Tris, 10% (v/v) acetic acid and 10 mM EDTA), containing 0.5 µg/mL Ethidium Bromide. The separation was held at 200 V in 0.25x TAE buffer and GeneRuler DNA Ladder Mix (Fermentas) was used as molecular marker. The DNA fragments were analysed under UV light. The DNA of interest was extracted and purified from the agarose gel using GenElute™ Gel Extraction Kit (Sigma-Aldrich), according to the manufacturer's instructions.

2.2.3. Cloning into pCR-Blunt vector

The blunt DNA fragments (AmutPSI_STP and AmutPSI_noSTP), obtained from the insertion of restriction enzyme adaptors through PCR, were subsequently cloned into pCR-Blunt vector (Zero Blunt Cloning Kit, Invitrogen), according to the manufacturer's instructions. The molar ratio between insert and vector was 5:1 and the amount of insert was calculated using the equation bellow. Competent *E. coli* were then transformed with the product of the ligations.

$$ng_{insert} = \frac{ng_{vector} \times bp_{insert}}{bp_{vector}} \times 5$$

2.2.4. Plasmid miniprep and enzymatic restriction screening

For screening purposes, plasmid DNA extraction from *E. coli* was performed by the boiling method. A single colony of transformed *E. coli* was inoculated in LB medium supplemented with kanamycin (50 µg/mL) and grown overnight at 37 ºC with 180 rpm orbital shaking. From the overnight culture, 1.5 mL were centrifuged 30 seconds at 14000 x g and cells were resuspended in 200 µL STET buffer (8% (w/v) sucrose, 0.1% (w/v) triton-100, 50

mM EDTA and 50 mM tris-HCl, pH 8.0), with 1.5 mg/mL lysozyme. After vortex homogenisation and a 5 minute incubation at room temperature, the cells were boiled for 45 seconds and centrifuged for 5 minutes at 14000 x g. The resulting pellet was removed using a toothpick and 200 µL of isopropanol was added for DNA precipitation. A gentle homogenisation preceded a 10 minute centrifugation at 14000 x g. The sediment was then washed with 200 µL 70% ethanol, air-dried and resuspended in 20 µL of ddH_2O supplemented with RNAseA.

Once the DNA was isolated from the *E. coli* cultures, AmutPSI_STP and AmutPSI_noSTP were screened for putative positives clones by restriction enzyme digestion, using the enzymes correspondent to the previously added adaptors. Thus, for AmutPSI_STP *XbaI* and *SacI* were used, and for AmutPSI_noSTP *XbaI* and *SalI* were used. The restriction reactions occurred according to the enzymes manufacturers' instructions and the results were analysed by agarose gel electrophoresis. The selected clones were confirmed by sequencing [M13 uni (-21) and M13 rev (-29) universal primers; Eurofins MWG Operon] prior to further cloning procedures.

2.2.5. Sub-cloning into pVKH18-En6

Once the sequences of AmutPSI_STP and AmutPSI_noSTP in pCR Blunt vector were confirmed, the DNA fragments were excised, using the restriction enzyme adaptors, and cloned into pVKH18-En6 (expression binary vector). The constructions were used to transform competent *E. coli* and, after DNA extraction, screening for positive clones by restriction analysis was performed, as previously described. One clone of each construction was used for the transformation of competent *A. tumefaciens*. Prior to *N. tabacum* leaf infiltration, the clones were screened once more by restriction analysis and only selected ones were further used.

2.2.6. Transient expression in *Nicotiana tabacum*

In an attempt to evaluate the expression and processing of AmutPSI_STP and AmutPSI_noSTP, *N. tabacum* leaves were infiltrated with *A. tumefaciens* cultures, as previously described. For AmutPSI_noSTP, *N. tabacum* leaves were similarly infiltrated and, at regular time points (3 and 6 days), leaf samples were analysed through CLSM. Concerning AmutPSI_noSTP, the analysis could not be performed in due time.

2.2.7. Expression analysis by CLSM

The expression and localisation of AmutPSI_noSTP were analysed through Confocal Laser Scanning Microscopy, after *N. tabacum* leaf infiltration. Leaf pieces of approximately 1 cm^2 were excised and placed on a glass plate with water, with the abaxial epidermis facing up. The images were acquired on a SP2 Leica Confocal Microscope (Leica Microsystems, Heidelberg) and the excitation wavelength used was 561 nm (for fluorescent protein mCherry).

2.3. Maintenance and transformation of bacterial strains used along the work

Two different types of bacteria were used during this project. *Escherichia coli* TOP10 was used due to its high efficiency rate of transformation and *Agrobacterium tumefaciens* LBA4404 was the chosen strain for the transient transformation of plant systems. Both strains were grown in Luria Bertani (LB) medium, with the addition of 1.5% (w/v) agar in case solid medium was needed. The cultures were grown at 37 ºC with 180 rpm orbital shaking for *E. coli* and at 28 ºC with 200 rpm orbital shaking for *A. tumefaciens*.

2.3.1. Preparation of competent *Escherichia coli*

For the preparation of competent *E.coli* TOP10 cells, one single colony was inoculated in 25 mL of LB medium and incubated overnight at 37 ºC with 180 rpm orbital shaking. The overnight culture was added to 225 mL of LB medium supplemented with 1 M $MgCl_2$ and 1 M $MgSO_4$. The culture was left to grow at 37 ºC with 180 rpm orbital shaking until $OD_{600} \approx 0.6$. The cells were placed on ice for 10 minutes before centrifugation of 25 mL aliquots at 775 x g for 5 minutes, at 6 ºC. The supernatant was then eliminated and the cells were resuspended in 100 mL of RF1 buffer (100 mM RbCl, 50 mM $MnCl_2.4H_2O$, 30 mM KAc, 10 mM $CaCl_2.2H_2O$, 15% (v/v) glycerol, pH 5.8, filter sterilised) and chilled on ice for 15 minutes, followed by centrifugation at 775 x g for 5 minutes, at 6 ºC. The supernatant was once more eliminated and the cells were resuspended in 16 mL of RF2 buffer (10 mM RbCl, 75 mM $CaCl_2$, 10 mM MOPS, 15% (v/v) glycerol, pH 8, filter sterilised). The suspension was divided in 400 µL/ 100 µL aliquots and stored at -80 ºC.

2.3.2. Transformation of *Escherichia coli*

The transformation of *E. coli* cells was performed by the heat shock method. Once thawed on ice, 100 µL of chemically competent cells were added to the whole volume of the DNA ligation, or to 1-2 µL of plasmid miniprep. After a 30 minutes incubation on ice, the mixture was subjected to a heat shock at 42 ºC for 90 seconds and then placed back on ice. The cells were then incubated at 37 ºC for 30 minutes with 300 µL of LB medium, before centrifugation at 775 x g for 2 minutes. 300 µL of the supernatant were eliminated and the cells were resuspended in the remaining volume. Finally, 100 µL of cells were plated onto LB-agar supplemented with the appropriate antibiotic. When using pBluescript II SK plasmid, a 50 µg/mL of ampicillin was applied, whereas a 50 µg/mL of kanamycin was applied when using pVKH18-En6 vector.

2.3.3. Preparation of electrocompetent *Agrobacterium tumefaciens*

One single colony of *A. tumefaciens* was inoculated overnight in 10 mL of LB medium, at 28 ºC with 200 rpm orbital shaking. The overnight culture was then added to 200mL of LB medium and grown at 28 ºC with until OD_{600} = 0.5-0.6. Prior to a 10 minute centrifugation at 3500 x g, the culture was divided for four 50 mL centrifuge tubes and the cells were chilled on ice for 30 minutes. The resulting pellet was resuspended in 100 mL of ice-cold 1mM HEPES buffer (pH 7.5, filter sterilised) and centrifuged once more for 10 minutes. Cells were subsequently resuspended in 50 mL of the previous utilised buffer supplemented with 10% (v/v) glycerol. In succession to a third centrifugation, the cells were resuspended in 1 mL of ice-cold 1mM HEPES buffer similarly supplemented with 10% (v/v) glycerol and 50 µL aliquots were stored at -80 ºC.

2.3.4. Transformation of *Agrobacterium tumefaciens*

The transformation of *A. tumefaciens* electrocompetent cells was performed by electroporation, method described by Wen and Forde (1989), since it shows to be more efficient than the heat shock method for this type of cells. After thawing on ice, 50 µL of competent cells were added to 10 µL of miniprep DNA and the mixture was transferred to a pre-chilled electroporation cuvette. The electroporation was held in a Micropulser Electroporator (BioRad), at 2.5 kV and 25 µF, with Pulse controller set to 100 Ω. Once the electroporation was performed, 1 mL of LB medium was immediately added to the cells and the mixture transferred to a 1.5 mL tube. Prior to plating onto LB-agar medium with selective antibiotic, the cells were incubated at 28 ºC for 4 hours without shaking.

3. RESULTS

3.1. Dissecting the role of the plant cell wall in the regulation of protein trafficking

For a better understanding of cardosins A and B sorting, secretion assays were performed for a number of constructions codifying these proteins, or part of them, using protoplasts isolated from transformed *N. tabacum* leaves. In an attempt to unveil the role of the cell wall in the trafficking of these proteins, this compartment was allowed to regenerate in the course of the experiment. Meanwhile, the cells were visualised at established time points through CLSM and samples were collected for biochemical studies.

3.1.1. Protoplast culture and cell wall regeneration optimisation

Numerous protocols for cell wall regeneration have been described in the literature (Horine & Ruesink 1972; Nagata & Takebe 1971; Balestri & Cinelli 2001); however, the regeneration process depends on several factors, such as light, agitation, temperature or culture medium, and these factors differ according to the type of plant used. Therefore, an optimisation of the process for *N. tabacum* protoplasts was required, considering the conditions available at the laboratory, aiming for a better planning of the subsequent assays.

For the optimisation of protoplast culture, as well as cell wall regeneration, protoplasts were isolated from non-transformed *N. tabacum* leaves, and placed on different culture media with different conditions of light, agitation and temperature. The viability of the cells was monitored through light microscopy and the regeneration of the cell wall was observed through fluorescence microscopy. To allow the visualisation of cell wall, a fluorescent stain – Calcofluor White ST – was used, which strongly binds to cellulose. As a result, the cell wall appeared coloured white under UV light, which made its identification possible.

Two different culture media were selected from the literature as the most adequate for the plants and culture conditions available – medium A and medium B. The culture conditions were tested with both media, with the same plant and at the same time. In this experiment the temperature was set to 22 ºC, which showed to be ideal for the protoplasts. Several combinations of lighting and agitation were tested, while the viability of the cells was monitored, as previously described. The viability of the protoplasts showed to be the most satisfactory when light and agitation were absent, as the presence of these factors lead to the formation of cell aggregates and early cell death. Once the culture conditions were settled, the most suitable culture medium for the cell wall regeneration was selected. Although the culture conditions were alike, the protoplasts placed in medium A (Fig 6 a, b, c) showed not to be as healthy as the ones placed in medium B, as the number of live cells observed in medium B was largely superior. Furthermore, the medium A, perhaps due to its

high sucrose content, showed to be more prone to contamination, which led to early death when compared to the alternative. In medium A, at the third day after protoplast isolation the formation of aggregates could be observed and few live cells were found, if any (data not shown). Contrastingly, when placed in medium B, the cells appeared to be healthy up to the sixth day after protoplast isolation (Fig 7 a-c, g-i).

The regeneration of cell walls was also more successful when the protoplasts were placed in medium B. In medium A, the formation of cell wall could not be observed, even when 24 hours had passed since protoplast isolation (Fig 6 d, e, f, red arrows) and it showed to be difficult to find healthy cells in the following days (data not shown). As for the protoplasts in medium B, cell wall formation could not be observed after 8 hours (Fig 7 d, e, red arrows), but after 24 hours a new cell wall was evident in most cells (Fig 7 f, yellow arrow). When 48h had passed since isolation, a new cell wall could be detected on the majority of the cells observed, which became increasingly evident as the days went by (Fig 7 j, k, l).

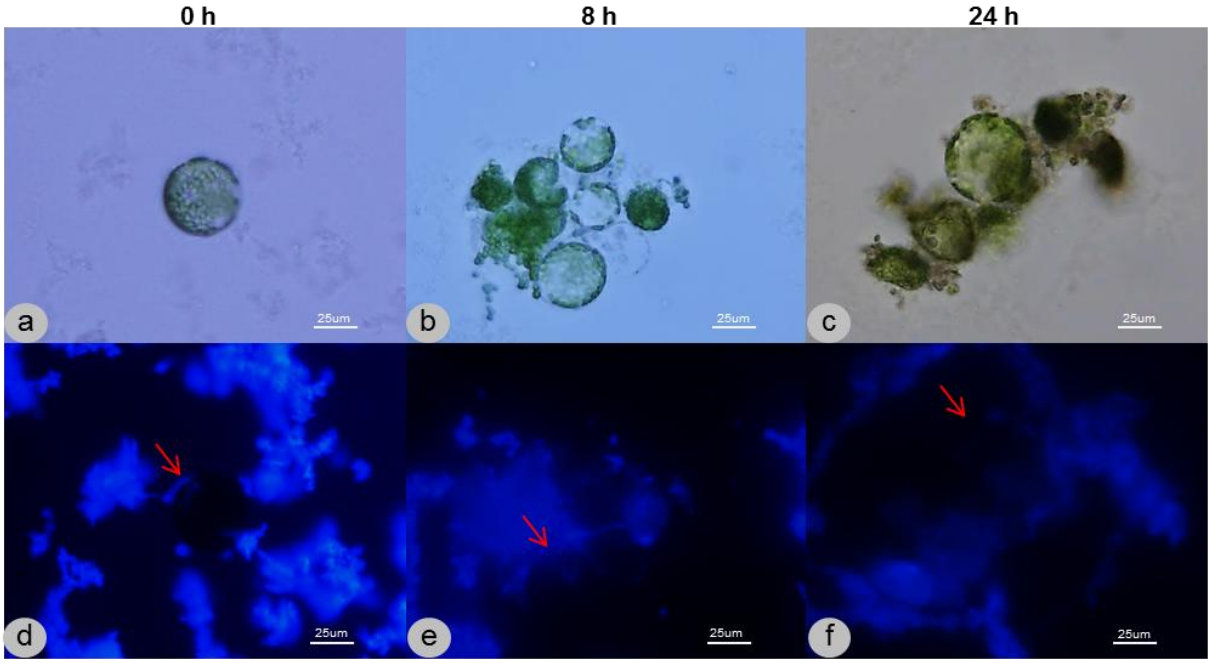

Figure 6 - Monitorisation of cell wall regeneration in *N. tabacum* protoplasts maintained in medium A.a, b, c - Light microscopy images; observations at various time points were performed in order to verify the viability of the cells. **d, e, f –** Fluorescence microscopy images; calcofluor white ST was added to the culture medium previously to the observations, in order to monitor the regeneration of new cell walls, by staining the cellulose. In medium A, the protoplasts appeared totally black, which indicates the lack of cell wall (red arrows).

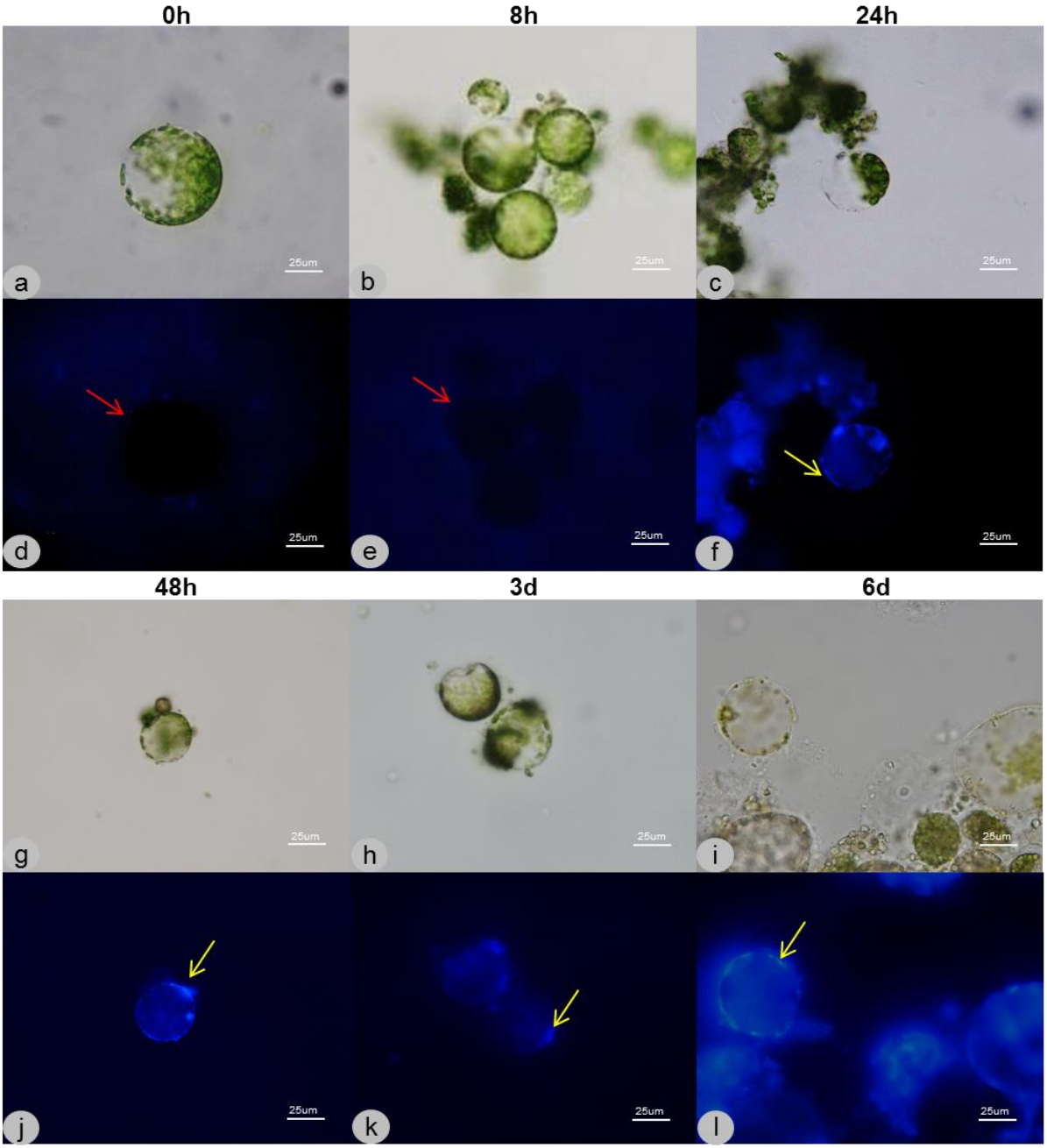

Figure 7 - Monitorisation of cell wall regeneration in *N. tabacum* protoplasts maintained in medium B.a, b, c, g, h, i - Light microscopy images; observations at various time points were performed in order to verify the viability of the cells. The protoplasts showed to be viable until 6 days after isolation (i). **d, e, f, j, k, l –** Fluorescence microscopy images; calcofluor white ST was added to the culture medium previously to the observations, in order to monitor the regeneration of new cell walls, by staining the cellulose. In medium B, the cells appeared totally black at the moment of isolation as well as 8 hours later (red arrows), which indicates lack of cell wall. However, 24 hours after protoplast isolation, a white fluorescence started to become visible at some points of the cell periphery, indicating the regeneration of a new cell wall (yellow arrow). As the days went by, more protoplasts regenerated a new cell wall (j, k, l, yellow arrows).

The optimisation of protoplast culture and cell wall regeneration showed to be essential for the planning of the secretion assays that followed, as the culture conditions and the life time of the cells were crucial information on which the success of the assays relied.

Hence, based on the optimisation, during the secretion assays the protoplasts were kept in medium B, at 22 ºC, in the dark and without agitation.

Regarding the establishment of the time points for sample collecting and observation in the secretion assays, the goal was to follow the evolution of the protein sorting from protoplast isolation until the regeneration of a new cell wall. As the formation of the cell wall seemed to take place from the eighth hour to the twenty fourth post protoplast isolation, the time points established for the secretion assays were 0h, 4h, 8h, 24h and 30h. These time points would allow the analysis of the protein localisation in protoplasts (0 – 4h), in protoplasts regenerating new cell walls (8 – 24h) and in cells which already regenerated a new cell wall (30h).

3.1.2. Analysis of cardosins' trafficking during protoplasting and cell wall regeneration

Protein secretion assays were performed as a way to better understand the trafficking of cardosins A and B, as well as to unveil a putative role for the cell wall within the sorting of these proteins, previously proposed (da Costa et al. 2010). Thus, *N. tabacum* leaves were agroinfiltrated and protoplasts were isolated from the transformed leaves and placed in medium B, at 22 ºC, in the dark and without agitation. Subsequently, the cells were observed through CLSM at the previously established time points, and cell and medium samples were collected separately for further biochemical analysis (SDS-PAGE followed by Western Blotting).

In *N. tabacum* protoplasts, the expression of cardosinA-mCherry was detected in the ER at 4h (Fig 8 b, pink arrow); however no signal was yet detected in some cells (Fig 8 g). Prior to 4h, no signal could be detected in any cell (Fig 8 a, f). From 8 to 30h, cardosin A seemed to accumulate in the vacuole in part of the protoplasts (Fig 8 c, d, e), although no signal could be observed in several cells, possibly indicating secretion (Fig 8 h, i, j). Contrastingly, in leaf, the expression could already be detected in the ER (Fig 8 k, l, m, pink arrows) and perinuclear ER (Fig 8 k, l, m, yellow arrows) at 0h and 4h, which might be due to a slower protein transport in protoplast when compared to the observed in leaf, as already described by Duarte et al. 2008. From 8h, a gradual protein accumulation in the central vacuole was observed in leaf, with a complete loss of ER pattern at 24h after isolation (Fig 8 j). In protoplasts, protein accumulation in the vacuole was detected from 8 to 30h after isolation (Fig 8 e, h, k), although lack of signal could also be observed in some cases (Fig 8 f, i, l), which could indicate secretion.

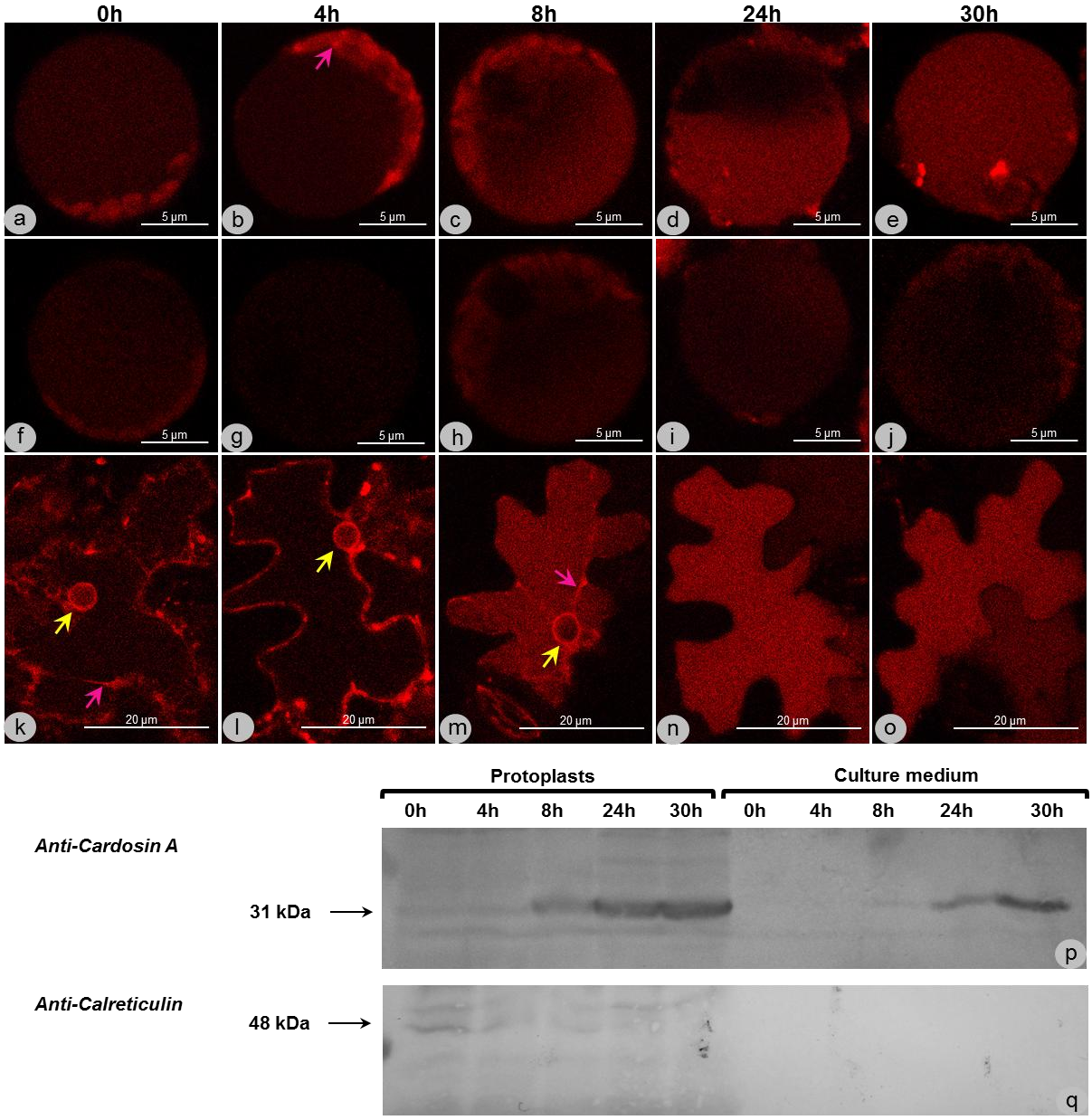

Figure 8 - Confocal microscopy images of *N. tabacum* mesophyll protoplasts and the respective leaf of origin, expressing cardosinA-mCherry during secretion assay and Western blot of the respective cell/medium protein fractions. The observations were performed at defined time points, for both protoplasts (a-j) and leaf (k-o) (0, 4, 8, 24 and 30 h from protoplast isolation). In protoplasts, no signal could be detected until 4h (a, f), when cardosin A could be detected in the ER (b, pink arrow); however no signal could yet be detected in some cells (g). From 8h to 30h, cardosin A could be detected in the vacuoles (c, d, e); however, no signal could be detected in several protoplasts (h, i, j), which could indicate secretion. In leaf, an ER pattern could be identified until 8 hours had passed (k, l, m), when protein accumulation in the central vacuole started to be detected (m). At 24 hours, the ER pattern had fully disappeared and the protein accumulated in the vacuole, maintaining its location at 30 hours (n, o). Protein samples were collected at the same time points as the confocal observations, separating the cells from the culture medium for Western blotting analysis (p). Using a specific antibody raised against cardosin A, the large subunit of cardosin A was detected in the cells' portion (31 kDa). In the culture medium portion, the large subunit of cardosin A was also detected increasingly from 8 to 30 hours after protoplast isolation, which could indicate secretion. Burst control was performed using an antibody raised against calreticulin and no detection was observed in the culture medium portion (q).

At the same time points as the observations through confocal microscopy, samples were collected from cells and culture medium, separately. The two fractions were analysed by Western blotting, using a specific antibody raised against cardosin A (Fig 8 p). The large subunit of cardosin A was detected in the protoplasts portion (31 kDa). In the culture medium portion, a secretion is detected between 8 and 30 hours. Burst control for the confirmation of secretion was performed by Western blotting, using an antibody raised against calreticulin and no detection was observed in the medium portion (Fig 8 q).

The results obtained for cardosinB-mCherry were similar to the ones already described for cardosin A. At the moment of protoplast isolation, as well as 4 hours later, the signal was quite low (Fig 9 a, b, f, g) and only detectable in the ER (Fig 9 b, pink arrow). As for cardosin A, from 8 to 30 hours the pattern of cardosin B expression varied from protein accumulation in the central vacuole (Fig 9 c, d, i) to low signal (Fig 9 e, h, j) and to accumulation in what might be the newly formed cell wall (Fig 9 j, blue arrow), which could indicate secretion. When observing the transformed leaf, an ER pattern could be detected at the moment of protoplast isolation, which was maintained until the twenty fourth hour (Fig 9 k-n), showing a slower transport when compared to cardosin A. From 24 hours, a gradual accumulation of protein in the central vacuole was clearly visible (Fig 9 n, o).

Cardosin B's large subunit was detected in the cells' portion by Western blotting (34 kDa), using an antibody raised against cardosin B. In the culture medium fraction, cardosin B is gradually secreted from 0 to 30 hours (Fig 9 p). Burst control for the confirmation of secretion was performed by Western blotting, using an antibody raised against calreticulin and no detection was observed in the medium portion (Fig 9 q).

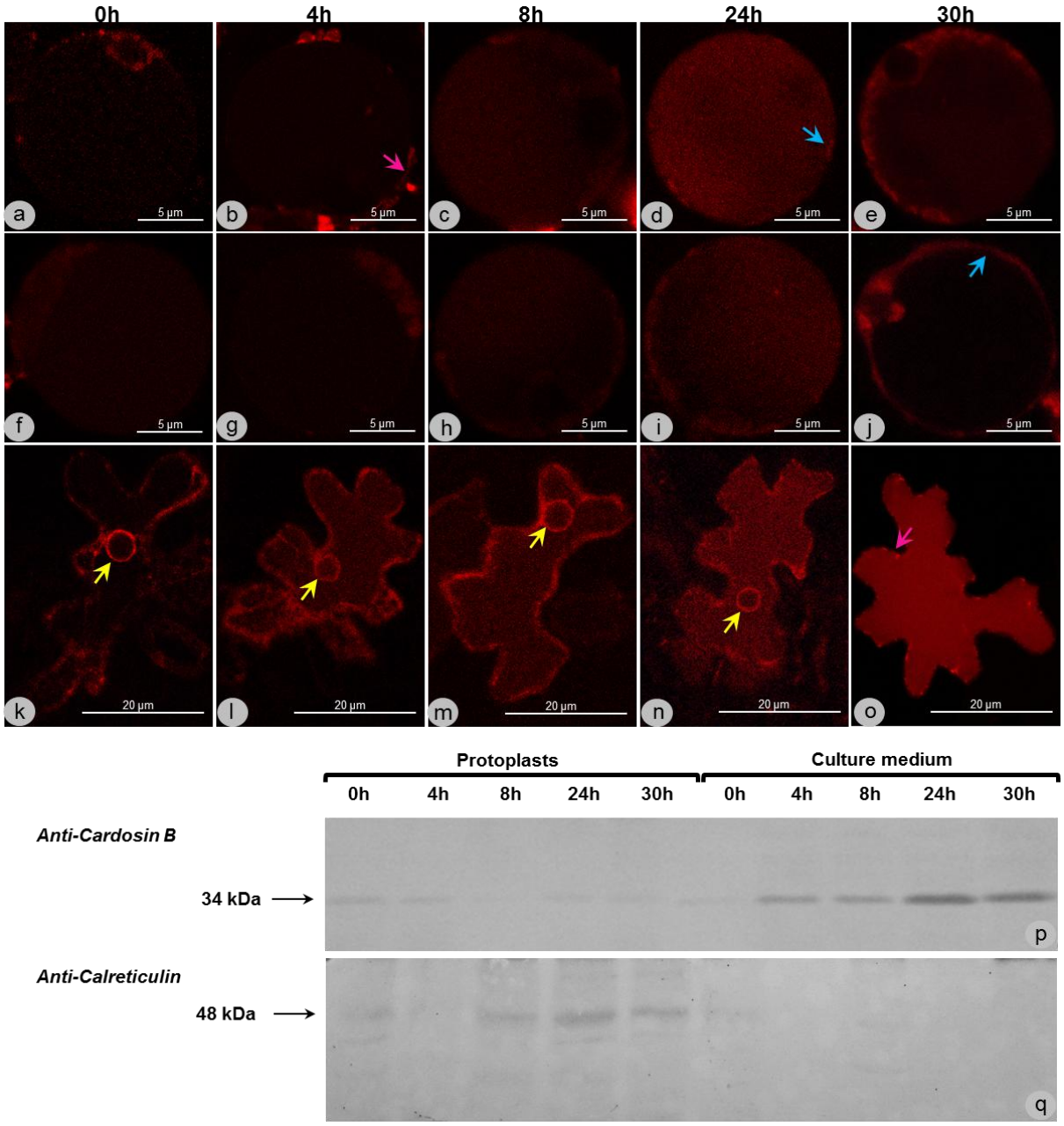

Figure 9 - Confocal microscopy images of *N. tabacum* mesophyll protoplasts and the respective leaf of origin, expressing cardosinB-mCherry, during secretion assay and Western blot of the respective cell/medium protein fractions. The observations were performed at defined time points, for both protoplasts (a-j) and leaf (k-o) (0, 4, 8, 24 and 30 h; from protoplast isolation). In protoplasts, fluorescence starts to be detected in the ER from 4 hours after protoplast isolation (b, pink arrow), although not in all cells (g), prior to which no signal could be observed (a, f). From 8 to 30 hours the signal pattern varied from protein accumulation in the central vacuole (c, d, i) to accumulation in what might be the new cell wall (j, blue arrow). There were also a few cases of lack of signal (e, h), which, along with the accumulation at the cell periphery at j, could indicate secretion. In leaf, the protein seemed to localise to the ER (k-o pink arrow) and perinuclear ER (k-n yellow arrow) from 0 to 24 hours, when a slight accumulation in the central vacuole started to show (n). When 30 hours had passed since protoplast isolation, cardosin B accumulated in the central vacuole in leaf (o). Using a specific antibody raised against cardosin B, the large subunit of cardosin B was detected in the cells' portion (34 kDa). In the culture medium portion, the large subunit was increasingly detected (p). Burst control was performed using an antibody raised against calreticulin and no detection was observed in the culture medium portion (q).

3.1.3. The role of C-terminal region in cardosins trafficking during protoplasting and cell wall reforming

The C-terminal is a vacuolar sorting determinant, not only for cardosins, but also for other known APs (Ramalho-Santos et al. 1998). This domain is known to direct the proteins to the lytic vacuole, through the Golgi, following the classic pathway for soluble proteins. As a way of unveiling the role of the C-terminal in the sorting of cardosins during protoplasting and cell wall regeneration, secretion assays were performed with *N. tabacum* protoplasts expressing mCherry-CTermA and mCherry-CTermB. Hence, *N. tabacum* leaves were agroinfiltrated and protoplasts isolated from the transformed leaves and placed in medium B, at 22 ºC, in the dark and without agitation. Subsequently, the cells were observed through CLSM at the previously established time points, and cell and medium samples were collected separately for further biochemical analysis (SDS-PAGE followed by Western Blotting).

From protoplast isolation to 4 hours, the C-terminal of cardosin A linked to mCherry was only detected in the perinuclear ER (Fig 10 yellow arrows) and ER network (Fig 10 pink arrows) in protoplasts (Fig 10 a, g) and the signal was too low to be detected in some cases (Fig 10 b, f). From 8 to 30 hours, a gradual accumulation of protein in the central vacuole was observed (Fig 10 c-e, j), although the ER pattern was kept throughout the assay (Fig 10 c, h-j, pink and yellow arrows). At 30h, a slight accumulation in the periphery of the cells could be observed, which could correspond to the newly formed cell wall (Fig 10 e, j, blue arrows) When analysing the transformed leaf, fluorescence detection laid in the ER from the moment of protoplast isolation until 24h (Fig 10 k-n, pink and yellow arrows), although it accumulated mainly in the central vacuole from 8 to 30 hours (Fig 10 m-o).

Through Western blotting (Fig 10 p), the C-terminal linked to mCherry was detected increasingly in the cells' portion from 0 to 30 hours (27 kDa). In the culture medium fraction, protein detection was successful from 4 to 30 hours, though in higher proportions at the last two time points of the secretion assay. Burst control for the confirmation of secretion was performed by Western blotting, using an antibody raised against calreticulin and no detection was observed in the medium portion (Fig 10 q).

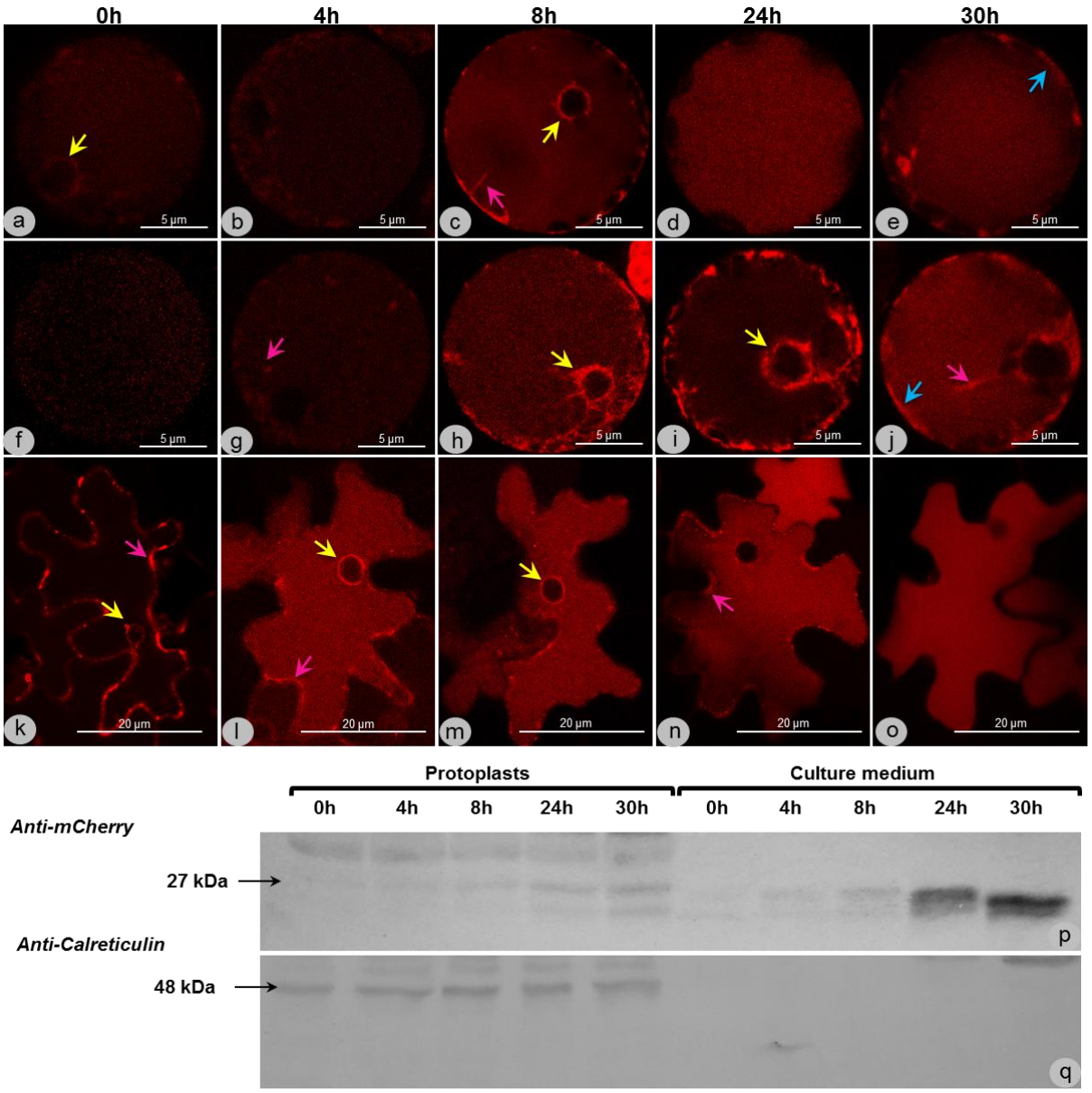

Figure 10 - Confocal microscopy images of *N. tabacum* mesophyll protoplasts and the respective leaf of origin, expressing mCherry-CTermA, during secretion assay and Western blot of the respective cell/medium protein fractions. The observations were performed at defined time points, for both protoplasts (a-j) and leaf (k-o) (0, 4, 8, 24 and 30 h; from protoplast isolation). Regarding the expression in protoplasts, the low signal detected until 4 hours had passed since protoplast isolation was mainly localised to the perinuclear ER (yellow arrows) and ER network (pink arrows) (a, b, f, g). The ER pattern was kept during the whole assay (c, h-j, pink and yellow arrows), although a gradual accumulation in the central vacuole was observed from 8 to 30 hours (c-e, j). In leaf, the C-terminal linked to mCherry was observed in the ER from protoplast isolation until 24 hours (k-n, yellow and pink arrows). Vacuole accumulation was visible at 4 hours and kept throughout the assay (l-o). By Western blotting (p), the C-terminal of cardosin A linked to mCherry was detected increasingly in the cells' fraction of the secretion assay, as well as in the culture medium portion from 4 to 30 hours (27 kDa). Burst control was performed using an antibody raised against calreticulin and no detection was observed in the culture medium portion (q).

Until 4 hours had passed since protoplast isolation, the C-terminal of cardosin B linked to mCherry was detected mostly in the ER network (pink arrows) and perinuclear ER (yellow arrows) (Fig 11 a, b, f, g). From 8 to 30 hours, protein accumulation in the vacuole was

observed (Fig 11 c, d, e), though the ER pattern was kept for most of the cells (Fig 11 c, d, h-j, pink and yellow arrows). Similarly, in leaf, the fluorescence was detected in the ER network throughout the assay (Fig 11 k-o, pink and yellow arrows). Between 8 to 30 hours, an accumulation of protein in the central vacuole is observed (Fig 11 m, n, o).

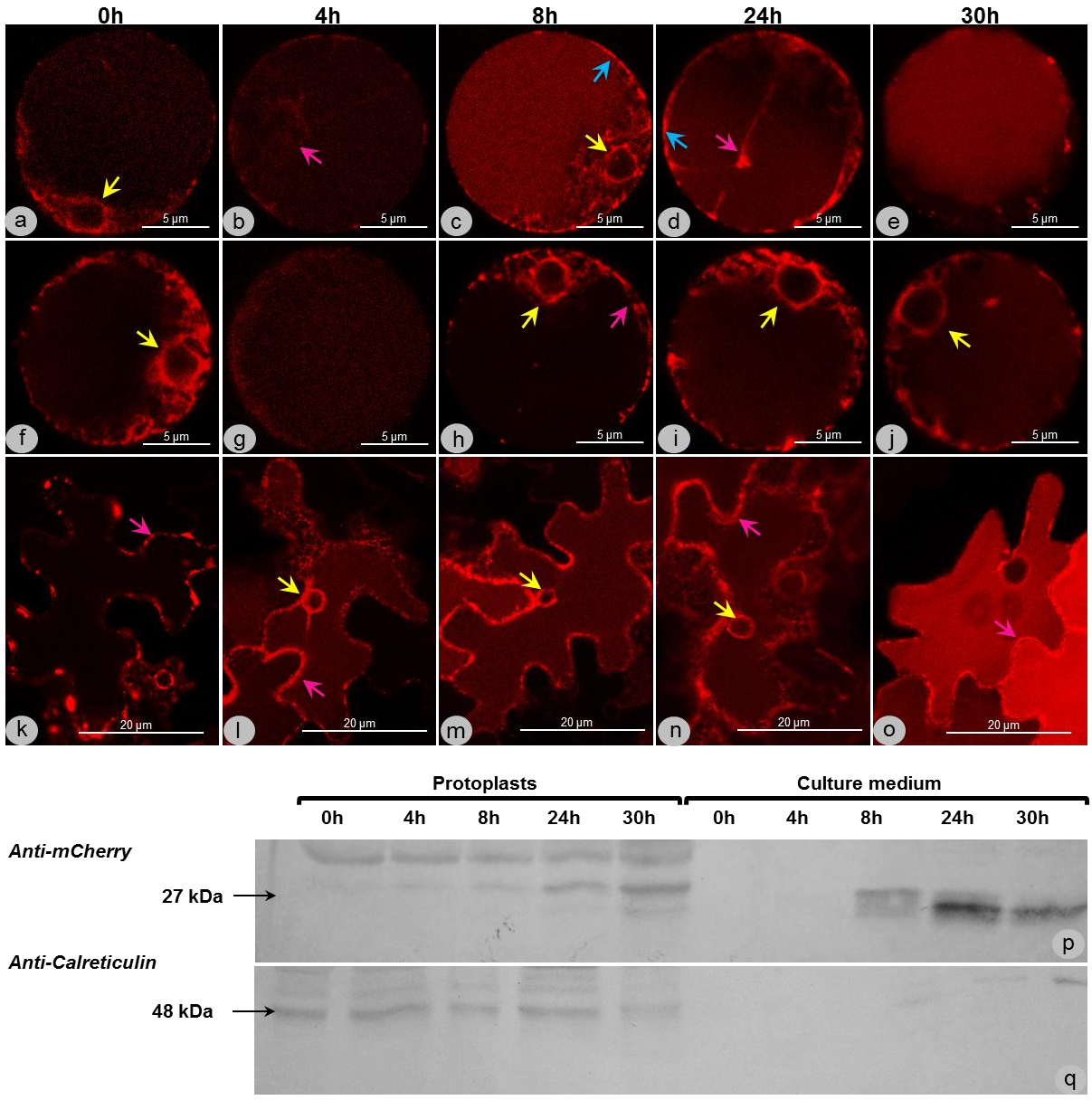

Figure 11 - Confocal microscopy images of *N. tabacum* mesophyll protoplasts and the respective leaf of origin, expressing mCherry-CTermB, during secretion assay and Western blot of the respective cell/medium protein fractions. The observations were performed at defined time points, for both protoplasts (a-j) and leaf (k-o) (0, 4, 8, 24 and 30 h; from protoplast isolation). In protoplasts, the C-terminal was mainly detected in the perinuclear ER (yellow arrows) and ER network (pink arrows) in the first 4 hours of the assay (a, b, f,). In a few cases, no signal was detected (g). At 8 hours, accumulation in the central vacuole was detected (c), which was kept through the following time points (d, e, I, j), although the ER pattern was constant during the whole assay in most cells (c, d, h-j, pink and yellow arrows). At 8 and 24h, some fluorescence accumulated in the periphery of the cells, in what seemed to be the newly formed cell wall (c, d, blue arrows). In leaf, the fluorescence detection localised mostly to the ER during the assay (k-o, pink and yellow arrows). From 8 to 30 hours, protein accumulation in the vacuole was detected (m-o). In the Western blot (p), detection of mCherry-CTermB was observed in the cells' portion (27

kDa), using an antibody raised against mCherry. The protein was detected in the culture medium fraction as well, from 8 to 30 hours. Burst control was performed using an antibody raised against calreticulin and no detection was observed in the culture medium portion (q).

Through Western blotting (Fig 11 p), and using an antibody raised specifically against mCherry, the mCherry-CTermB was detected in the cells' fraction, gradually increasing its proportion during the assay. The protein was also detected in the last three time points of the assay in the culture medium portion. Burst control for the confirmation of secretion was performed by Western blotting, using an antibody raised against calreticulin and no detection was observed in the medium portion (Fig 11 q).

3.1.4. The role of PSI domain in cardosins trafficking during protoplasting and cell wall reforming

The PSI works as a vacuolar sorting determinant both for cardosin A and cardosin B. However, recent studies in our lab have shown that the two PSI regions use different intracellular routes towards the vacuole. While cardosin A PSI bypasses the Golgi, cardosin B PSI follows a Golgi-dependent route (Pereira et al. 2012, submitted). In an attempt to clarify if this difference in the PSIs is related to the behaviour of cardosins during protoplasting and following cell wall regeneration, the same experiment performed for cardosins A and B was executed for the isolated cardosins' PSI regions fused to mCherry. Thus, *N. tabacum* leaves were agroinfiltrated with PSIA-mCherry and PSIB-mCherry and protoplasts were isolated from the transformed leaves and placed in medium B, at 22 ºC, in the dark and without agitation. Subsequently, the cells were observed through CLSM at the previously established time points, and cell and medium samples were collected separately for further biochemical analysis (SDS-PAGE followed by Western blotting).

At the fourth hour after protoplast isolation, PSIA-mCherry became detectable in protoplasts mostly in the perinuclear ER (Fig 12 b, g, yellow arrows), prior to which no signal could be observed (Fig 12 a, f). Between the eighth and the twenty fourth hours, an accumulation of protein in the central vacuole started to be evident (Fig 12 c, d, h). Despite the fact that the perinuclear ER pattern was visible from 4 to 30 hours since protoplast isolation (Fig 12 b-d, g-j, yellow arrows), most cells showed accumulation in the central vacuole with no detection in the ER at 30h (Fig 12 e). In leaf, the perinuclear ER was observed throughout the assay (Fig 12 k-n, yellow arrows), decreasing in intensity only at the

30h time point, when a slight ER pattern was detected (Fig 12 o, pink arrow). A slight accumulation in the central vacuole was detected at 4 hours, increasing gradually during the assay (Fig 12 l-o).

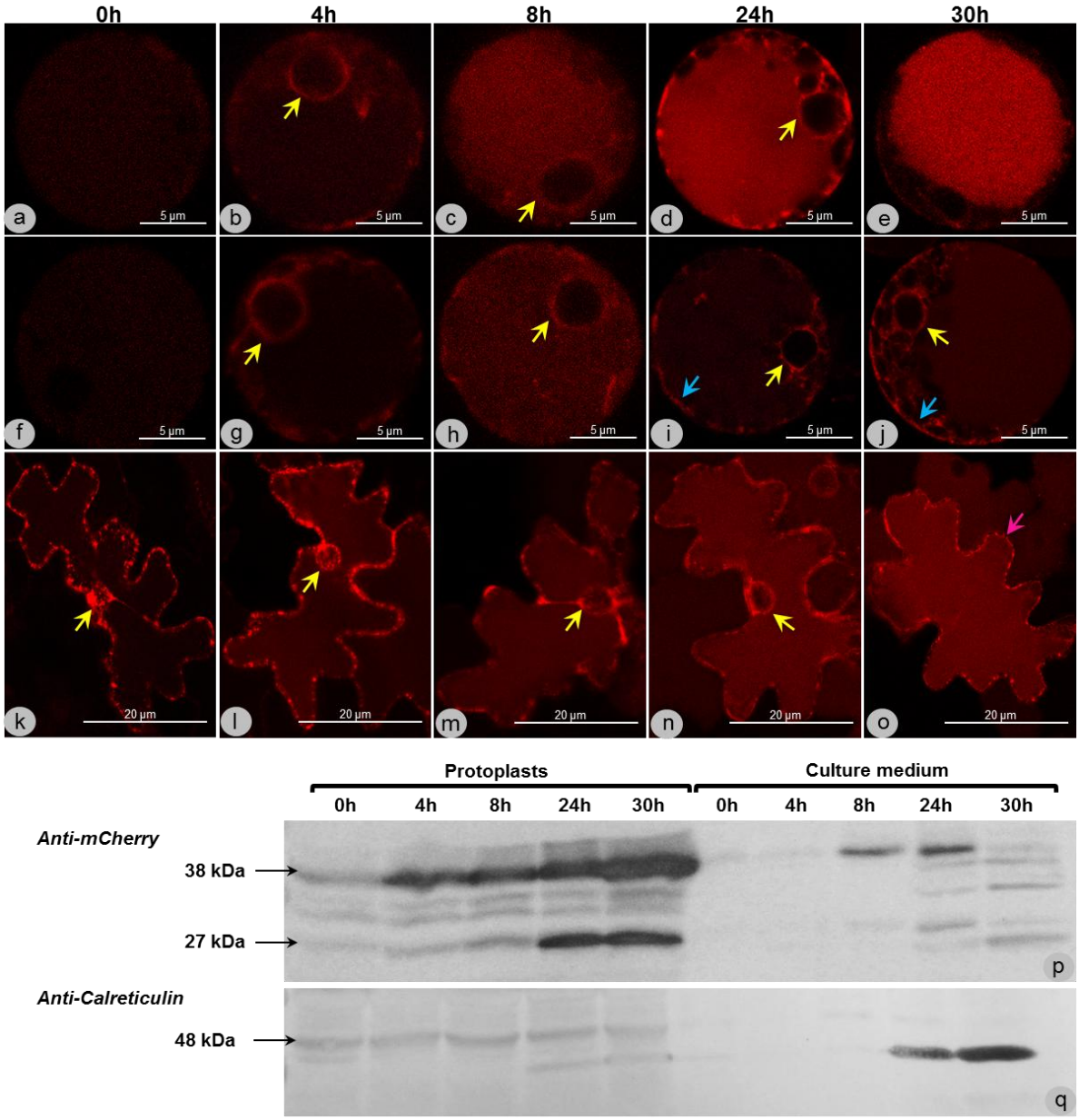

Figure 12 - Confocal microscopy images of *N. tabacum* mesophyll protoplasts and the respective leaf of origin, expressing PSIA-mCherry, during secretion assay and Western blot of the respective cell/medium protein fractions. The observations were performed at defined time points, for both protoplasts (a-j) and leaf (k-o) (0, 4, 8, 24 and 30 h; from protoplast isolation). In protoplasts, the PSI domain was first detected in the perinuclear ER when 4 hours had passed since protoplast isolation (b, g, yellow arrows), prior to which no signal was detected (a, f). From 8 to 24 hours, the ER pattern was still visible, although some accumulation in the central vacuole was detected (c, d, h, I, yellow arrows) and in what could be the new cell wall (I, blue arrow). At 30 hours, the PSI linked to mCherry had accumulated in the vacuole in most cells (e), in spite of being detected in the ER in a few protoplasts (j, yellow arrow) and in what seemed to be the newly formed cell wall (j, blue arrow). In leaf, the PSIA-mCherry localised to the ER network and perinuclear ER until 24 hours had passed (k-n, yellow arrows). A slight accumulation in the central vacuole was detected at 4 hours (l), which increased gradually during the assay (m-o). At 30 hours, the protein was mainly accumulated in the vacuole, though some still localised to the ER network (o, pink

arrow). Through Western blotting (p), the PSI domain of cardosin A linked to mCherry was detected in the cells' fraction, using an antibody raised against mCherry (38 kDa). A dissociated form of the fluorescent protein was also detected in the cells' portion of the secretion assay (27 kDa). In the culture medium, the PSIA-mCherry could be identified at the 8 and 24h time points analysed (38 kDa). Burst control was performed using an antibody raised against calreticulin and no detection was observed in the culture medium portion (q).

By Western blotting (Fig 12 p), the PSI of cardosin A linked to mCherry was detected increasingly in the cells' fraction (38 kDa), as well as the dissociated form of mCherry (27 kDa), using a specific antibody raised against the fluorescent protein. In the culture medium fraction, the PSI domain linked to mCherry was also detected (38 kDa), though only in the 8 and 24 h time points. Although the antibody used was specific for mCherry, a few bands were detected which appeared to be non-specific. Nonetheless, it might also be the case that these detections were actually specific, but yet to be identified in future developments of this study. Burst control for the confirmation of secretion was performed by Western blotting, using an antibody raised against calreticulin and no detection was observed in the medium portion (Fig 12 q).

Immediately after protoplast isolation, as well as 4 hours later, the PSI domain of cardosin B linked to mCherry was detected in the ER network (Fig 13 f, g, pink arrows) and perinuclear ER in protoplasts (Fig 13 a, g, yellow arrows), similarly to the observed in leaf (Fig 13 k, l, pink and yellow arrows). At 4h, there were some cases of protoplasts in which no signal could be observed (Fig 13 b). In protoplasts, in addition to the detected ER pattern in some cells (Fig 13 h, yellow arrow), an accumulation of protein in the central vacuole was detected at 8 hours (Fig 13 c, h), which increased gradually throughout the assay (Fig 13 c, d, i, j), similarly to the detected in leaf (Fig 13 m-o). Despite the accumulation in the vacuole, the ER pattern is kept in protoplasts and leaf during the assay, even when 30 hours had passed since the isolation of protoplasts (Fig 13 e, j, o, yellow arrows). Some fluorescence accumulated in the periphery of the protoplasts at 24 and 30 hours could correspond to newly formed cell wall (Fig 13 d, e, j blue arrows).

By Western blotting (Fig 13 p) and using a specific antibody raised against mCherry, PSIB-mCherry was detected in the cells' fraction of the secretion assay (38 kDa), as well as a dissociated form of the fluorescent protein (27 kDa). Regarding the culture medium portion, the PSI region linked to mCherry could not be detected. Burst control for the confirmation of secretion was performed by Western blotting, using an antibody raised against calreticulin and no detection was observed in the medium portion (Fig 13 q).

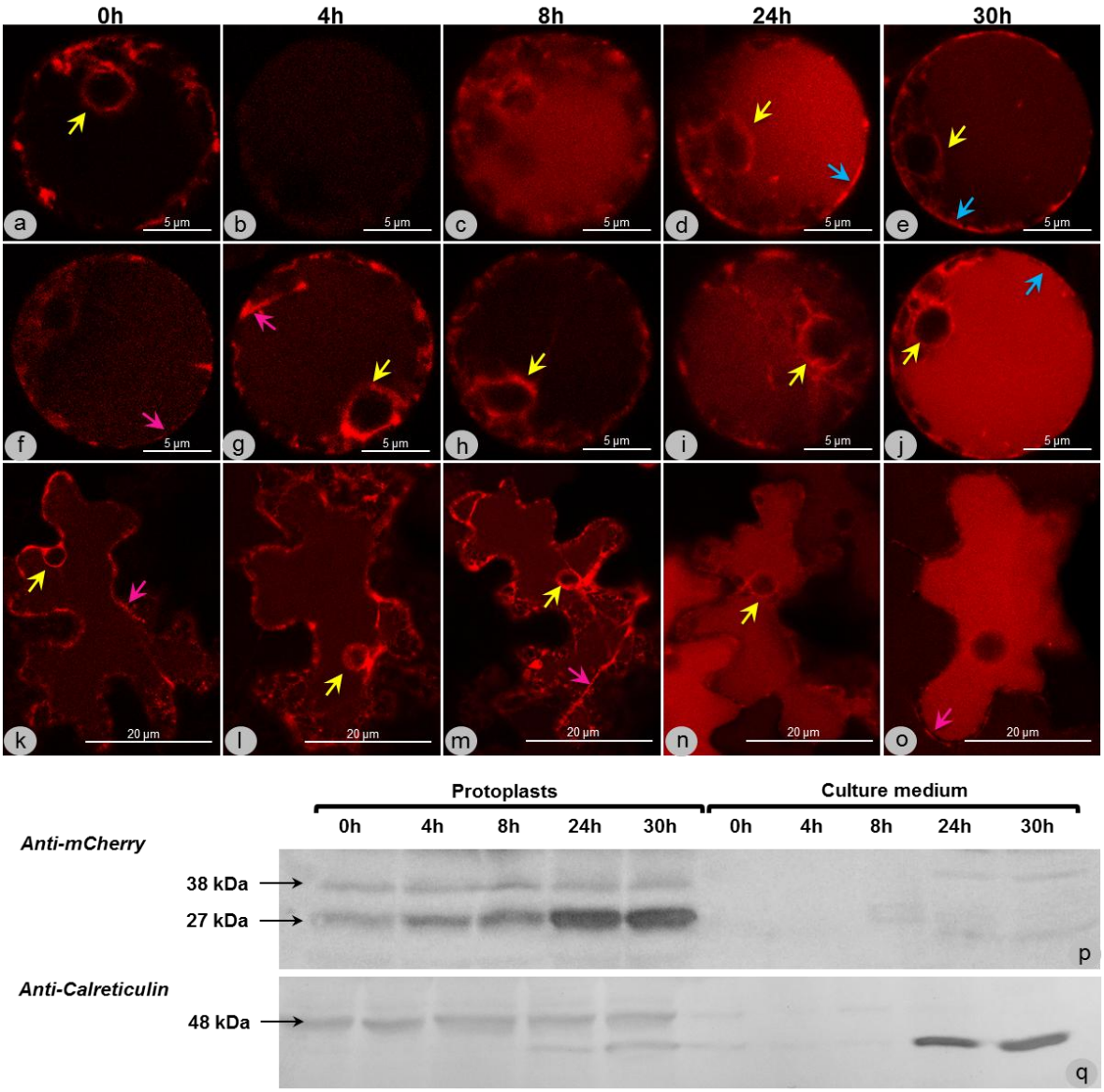

Figure 13 - Confocal microscopy images of *N. tabacum* mesophyll protoplasts and the respective leaf of origin, expressing PSIB-mCherry, during secretion assay and Western blot of the respective cell/medium protein fractions. The observations were performed at defined time points, for both protoplasts (a-j) and leaf (k-o) (0, 4, 8, 24 and 30 h; from protoplast isolation). In protoplasts, as in leaf, PSIBmCherry was detected in the ER network (pink arrows) and perinuclear ER (yellow arrows) from protoplast isolation, as well as 4 hours later (a, f, k, b, g, l). When 8 hours had passed, a slight accumulation in the central vacuole was detected, which increased gradually during the assay (c-e, h-j, m-o), although the protein was always detectable in the ER (yellow and pink arrows) in protoplasts and in leaf. By Western blotting and using a specific antibody raised against mCherry, PSIB-mCherry was detected in the cells' fraction of the secretion assay (p, 38 kDa). The dissociated form of mCherry was also detected in cells (27 kDa). In the culture medium, the PSI domain linked to mCherry could not be detected. Burst control was performed using an antibody raised against calreticulin and no detection was observed in the culture medium portion (q).

To simplify the interpretation, the results obtained throughout the secretion assays are summarised in the table below (Table 7). The data collected along this study points to a secretion of cardosin A and cardosin B upon protoplasting that does not occur in the leaf tissues. It is also clear that mCherry fused to cardosins C-terminal peptides should follow a similar pathway. However, probably because it directs proteins to the vacuole using different mechanisms, the PSI regions do not cause secretion of mCherry in this system.

Table 7 - Summary of the results obtained on the secretion assays performed, comprising the observations made through CLSM and Western blotting.

	Protoplasts	**Leaf**
Cardosin A	Vacuole/**Secreted**	Vacuole
Cardosin B	Vacuole/**Secreted**	Vacuole
C-terminal A	Vacuole/**Secreted**	Vacuole
C-terminal B	Vacuole/**Secreted**	Vacuole
PSI A	Vacuole	Vacuole
PSI B	Vacuole	Vacuole

3.2. Unveiling the role of the PSI domain in the regulation of cardosin A trafficking

In an attempt to better understand the role of the PSI domain in the regulation of cardosin A trafficking, point mutations were inserted at the cleavage sites of this domain in order to impair its removal during protein processing. Therefore, specific modified primers were designed for each cleavage site and site-directed mutagenesis was performed by PCR reaction, in order to mutate the 3' site. Following sequencing confirmation, the product of the first reaction was used as template for the mutation of the 5' site through PCR reaction, which was also confirmed by sequencing, after *E.coli* transformation and DNA extraction (Fig 14).

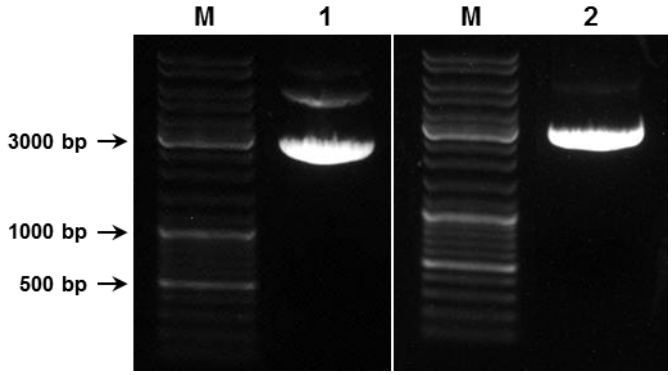

Figure 14 - Agarose gel electrophoresis of plasmid miniprep obtained from site-directed mutagenesis of PSI cleavage sites. 1 – Cardosin A mutated in the 3' cleavage site of the PSI domain, inserted in pBluescript II SK (3500 bp, miniprep supercoiled form); **2 –** Cardosin A mutated in both cleavage sites of the PSI domain, inserted in pBluescript II SK (3500 bp, miniprep supercoiled form); **M –** GeneRuler™ DNA Ladder Mix (Fermentas).

In order to facilitate the following cloning steps, restriction enzyme adaptors were added to the mutated cardosin A by PCR reaction. Two different constructions were assembled, AmutPSI_STP and AmutPSI_noSTP. While the first one became flanked by *XbaI* and *SacI* restriction enzyme adaptors, to the latter one *XbaI* and *SalI* restriction enzyme adaptors were added (Fig 15). Moreover, to AmutPSI_noSTP the stop codon was removed, in order to allow its sequence to become in frame with mCherry, when cloned into pVKH18-En6 expression binary vector, in the last cloning steps. The fusion of AmutPSI_noSTP with mCherry would be essential for further expression analysis of the protein by confocal microscopy.

The products of the latter PCR reactions were then cloned into pCRBlunt vector, followed by *E.coli* transformation, plasmid DNA extraction and confirmation by enzymatic restriction analysis and sequencing (Fig 16).

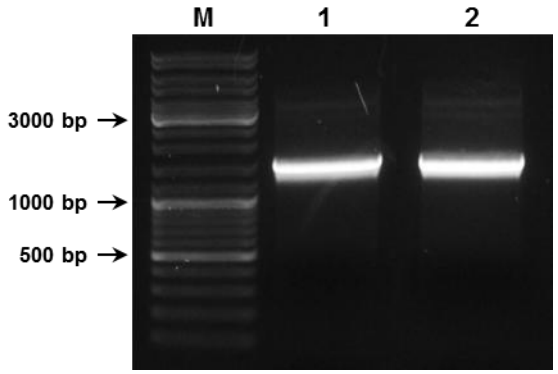

Figure 15 - PCR products from restriction enzyme adaptors addition on AmutPSI_STP and AmutPSI_noSTP. 1 – AmutPSI_STP – PCR product; mutated cardosin A with *XbaI* and *SacI* restriction enzyme adaptors (1500 bp); **2 –** AmutPSI_noSTP – PCR product; Mutated cardosin A with *XbaI* and *SalI* restriction enzyme adaptors (1500 bp); **M –** GeneRuler™ DNA Ladder Mix (Fermentas).

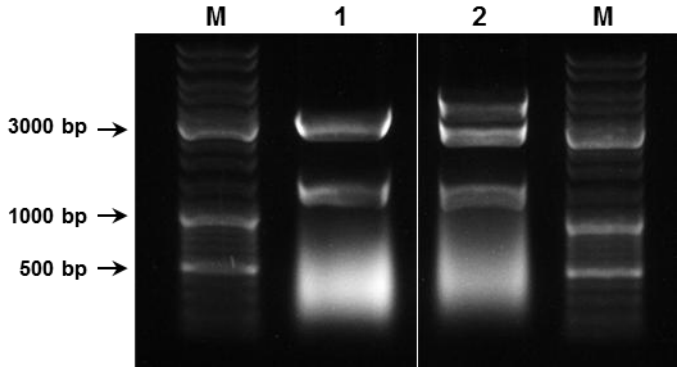

Figure 16 - Restriction analysis of AmutPSI_STP and AmutPSI_noSTP after insertion into pCRBlunt vector. **1 –** AmutPSI_STP in pCRBlunt vector digested with *XbaI* and *SacI* (pCRBlunt 3500bp; AmutPSI_STP 1500 bp); **2 –** AmutPSI_noSTP in pCRBlunt vector digested with *XbaI* and *SalI* (pCRBlunt 3500bp; AmutPSI_noSTP 1500 bp), partially non-digested; **M –** GeneRuler™ DNA Ladder Mix (Fermentas).

Once the restriction enzyme adaptors were in place, both AmutPSI_STP and AmutPSI_noSTP were enzymatically excised from pCRBlunt, using the added adaptors, and cloned into pVKH18-En6. The screening was performed through enzymatic restriction analysis (Fig 17).

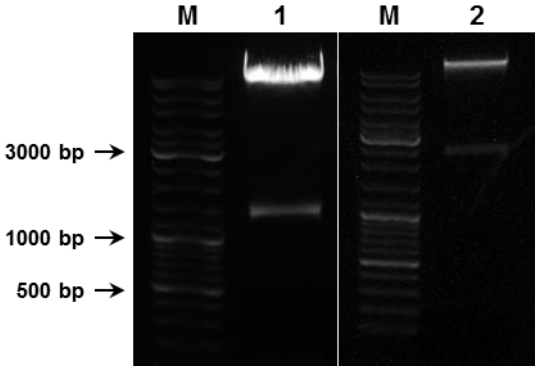

Figure 17 - Restriction analysis of the insertion of AmutPSI_STP and AmutPSI_noSTP into pVKH18-En6 vector. 1 – AmutPSI_STP in pVKH18-En6 vector digested with *XbaI* and *SacI* (pVKH18-En6 14000bp; AmutPSI_STP 1500 bp); **2 –** AmutPSI_noSTP in pVKH18-En6 vector digested with *XbaI* and *SalI* (pVKH18-En6 14000bp; AmutPSI_noSTP 2200 bp); **M –** GeneRuler™ DNA Ladder Mix (Fermentas).

The constructions AmutPSI_STP and AmutPSI_noSTP inserted in pVKH18-En6 expression binary vector were subsequently used for the transformation of *A. tumefaciens*. Henceforth, as AmutPSI_noSTP was already inserted into pVKH18-En6 and therefore in frame with mCherry, it was named AmutPSICh, while AmutPSI_STP was termed AmutPSI (Fig 18).

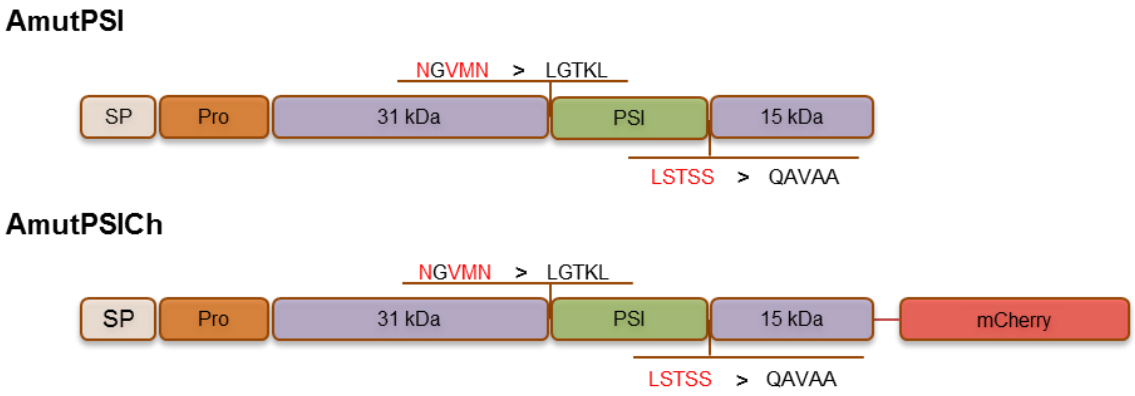

Figure 18 - Schematic representation of AmutPSI and AmutPSICh constructions. Flanking the PSI domain, the aminoacidic sequences of the cleavage sites are represented. The altered aminoacids are marked in red in the original sequence, on the left.

N. tabacum leaves were then agroinfiltrated and the expression of the constructs could be studied, through Western blotting for AmutPSI and through confocal microscopy for AmutPSICh. In this project, the analysis through Western blotting could not be performed in due time, contrastingly to the confocal microscopy, in which several aspects of AmutPSICh expression were perceived. The expression and localisation of AmutPSICh was observed three and six days after *N. tabacum* leaf infiltration (Fig 19 a-d). For control purposes, cardosinA-mCherry observations at the third day after *N. tabacum* leaf infiltration are also presented (Fig 19 e, f).

On the third day after leaf infiltration, the expression of AmutPSICh showed to be low and a pattern of round-shaped compartments could be observed at the periphery of most cells. The latter could also be detected on the differential interference contrast (DIC) images as small vesicles (Fig 19 a, b; yellow arrows). There is some fluorescence detected in the central vacuole, though in minor extent comparing to what could be observed for cardosinA-mCherry (Fig 19 a, e), which could indicate that the mutations on the PSI domain cleavage sites might implicate a slower transport of the protein through the secretory pathway. At the sixth day after infiltration, a slight increase in the protein accumulation in the vacuole could be verified, yet minor when compared to cardosinA-mCherry (Fig 19 c, e). The round-shaped compartments observed at the third day were reduced at the sixth day, in number as in size (Fig 19 c, d, yellow arrow).

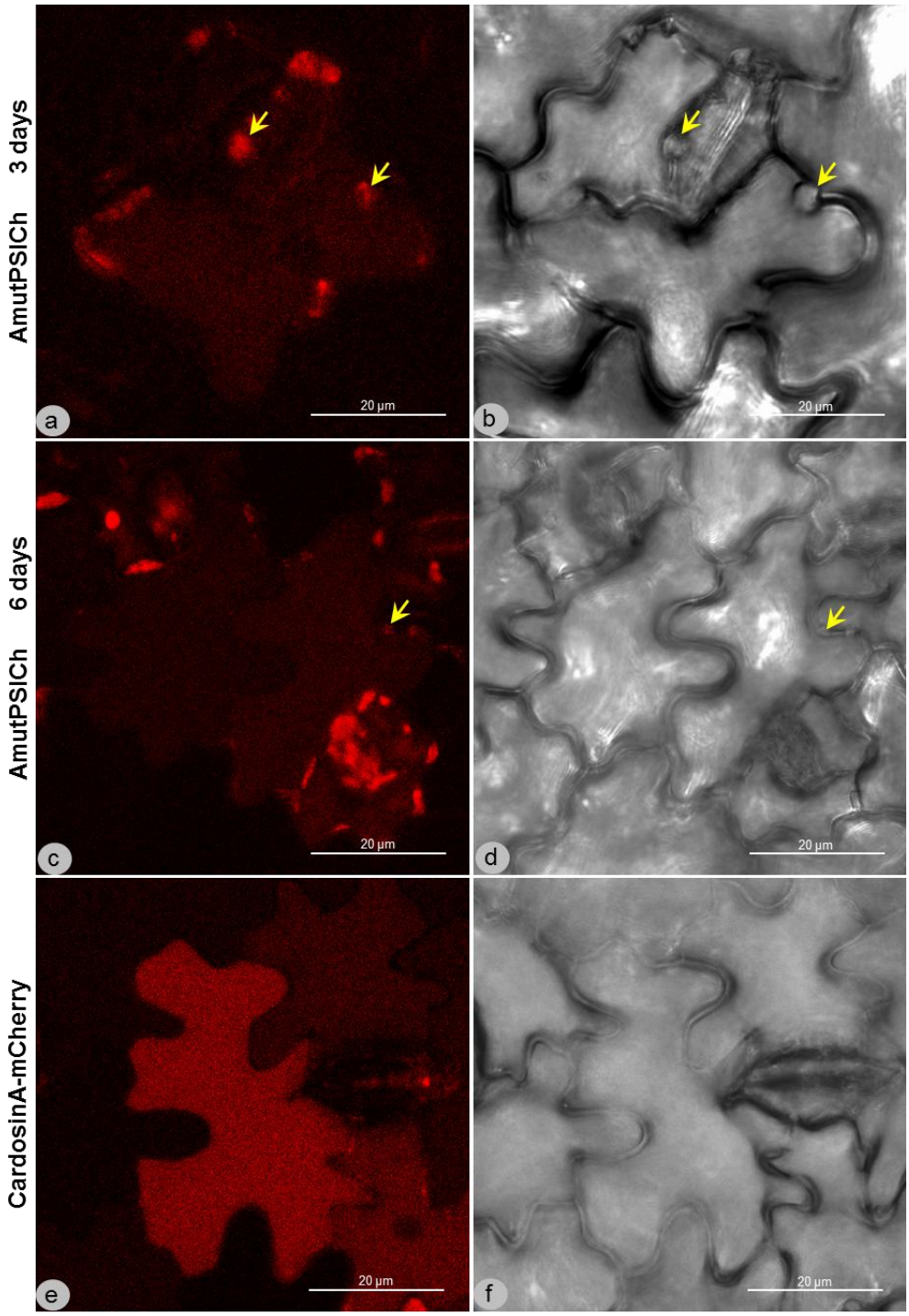

Figure 19 - Confocal microscopy images of *N. tabacum* leaves expressing AmutPSICh three and six days after agroinfiltration, and cardosinA-mCherry three days after agroinfiltration. Low expression was observed for AmutPSICh at both third (a) and six days (c) after infiltration. Accumulation in the central vacuole could be detected for AmutPSICh (a, c); however in a quite lower extent when compared to the non-mutated cardosin A (e). Round-shaped compartments were observed at the third day after infiltration and also three days after, in a lower extent (a, c, yellow arrows). The images on the right (b, d, f) represent the DIC images, on which the round-shaped compartments could be detected in the periphery of the cells (b, d, yellow arrows).

4. DISCUSSION

The main objective of this study was to understand the role of the cell wall in the regulation of protein sorting to the vacuole, using as base line previous results from our group of investigation. *N. tabacum* protoplasts expressing cardosins A and B fused to mCherry, as well as their VSDs also fused to mCherry were set as experimental models. As second aim, we proposed to optimise *N. tabacum* protoplast culture and cell wall regeneration process. Regarding the PSI domain from cardosin A, due to its intriguing features, we wanted to better understand its maturation and its role on cardosin A sorting. The chosen experimental strategies, as well as main results, are discussed below.

4.1. Dissecting the role of the plant cell wall in the regulation of protein trafficking

N. tabacum protoplasts regenerate a cell wall as early as 24h upon isolation

Protoplast transformation is a convenient system commonly used for a long time in developmental studies, evaluation of the effects of stress factors, cell wall biogenesis studies, intracellular localisation of proteins or protein interaction. The use of protoplasts is also very reliable, as they tend to reflect the targeting of the proteins in the intact tissue (Faraco et al. 2011). Protein trafficking studies are a popular use for *N. tabacum* protoplasts, as well as secretion assays for the study of sorting signals, although care must be taken as to avoid overexpression artefacts and mistargeting (Denecke et al. 2012). For studying the role of the cell wall in the regulation of cardosins' sorting, regeneration of the cell wall during the secretion assays was necessary. The process of regeneration, although being a natural process, ought to be carefully planned and optimised. The success of the regeneration process depends on several vital factors, among which the healthy condition of the plant material used, the culture conditions and the use of an appropriate culture medium. The process varies in time and culture requirements depending on the starting material from which protoplasts are isolated from, and the variation is even higher when bacteria or algae are used (Hahne et al. 1983). From the moment of isolation until the formation of a new cell wall, the protoplasts are fragile and osmotically unstable. Hence, it is essential that the culture medium used has the adequate composition to ensure the viability of the cells, including the use of a good plasmolyticum, such as mannitol or sucrose (Robinson & Schlösser 1978). In this work, two different media and different culture conditions were tested. Results show that medium B, mannitol enriched, gives the best results in terms of viability and cell wall regeneration. The advantage of medium B over medium A might have been the use of mannitol instead of sucrose, as the latter is highly prone to contamination and probably does not offer as much osmotic protection as mannitol. The same temperature

used for the maintenance of *N. tabacum* plants was set for the protoplast culture, which showed to be adequate. Perhaps due to the fragility of the protoplasts, for lack of support from a cell wall, even the weakest orbital agitation showed to be harmful for the cells in culture, reason why the protoplasts were henceforth maintained with no agitation. The same situation arose for the light; different light situations were tested and the best viability and cell wall regeneration were registered when the culture was kept in the dark. The viability of the cells in culture was monitored regularly through light microscopy and the regeneration of new cell walls was observed 24 hours after protoplast isolation, under a fluorescence microscope, by means of a fluorescent stain that strongly binds to cellulose – Calcofluor White ST. Although this stain has been proven not to be toxic to protoplasts (Hahne et al. 1983), it was only added to the cells a few minutes prior to observation, to avoid any cell stress. The data acquired during the optimisation process was crucial for the planning of the secretion assays that followed.

Cardosins A and B became secreted upon protoplasting

Previous results in our group have shown that cardosin B is accumulated in the lytic vacuole when expressed in *N. tabacum* leaves; however when protoplasts are isolated from the transformed leaves, the protein is secreted (da Costa et al. 2010). The intriguing results from those experiments made us pursue the hypothesis that the secretion might be a result of lack of some form of regulation from the cell wall. Hence, secretion assays were repeated for cardosin B and also executed for cardosin A. *N. tabacum* protoplasts derived from transformed leaves were used for the secretion assays and the analysis was performed through CLSM and Western blotting. At the time points determined during the protoplast culture optimisation (0, 4, 8, 24 and 30 hours), the transformed cells were observed by confocal microscopy and samples were taken from the culture, separating the cells from the medium for further biochemical analysis. At the same time, the leaves from which the protoplasts were isolated were also observed through CLSM, as an expression control. Burst controls were performed for cardosin A and B, using an antibody raised against calreticulin, an ER resident protein, and no signal was detected in the medium fractions.

Both cardosins are thought to follow a classical route to the lytic vacuole (Duarte et al. 2008; da Costa et al. 2010; Pereira et al. 2012, submitted). Cardosins enter the secretory pathway through the ER, by the presence of an N-terminal signal peptide. Mediated by COPII vesicles, the proteins are directed to the Golgi apparatus, from where they are delivered to the lytic vacuole, through the PVC/MVB. As expected, cardosin A and cardosin B are both vacuolar in *N. tabacum* leaves. However, when protoplasts were isolated from the transformed leaves, both cardosins were partially secreted to the culture medium, as

confirmed by the detection of their large subunits (31 kDa for cardosin A; 34 kDa for cardosin B) in the culture medium by Western blotting, using antibodies specifically raised against each cardosin. It was proposed by Duarte et al. (2008) that the complete processing of cardosin A requires the secretion of the 35 kDa intermediate form (Pro-segment + large subunit), followed by endocytosis from the apoplast and final accumulation in the lytic vacuole. According to the results here presented and data available from parallel studies, it seems that in intact leaves this processing step must occur in a very fast way, as through CLSM it is never detected any fluorescent signal in the cell periphery. However, this event may be enhanced after protoplasting due to the absence of the cell wall, which lead us to propose a working model (Fig 20). We consider that the secretion of cardosins in protoplasts is due to a lack of regulation from the absent cell wall. Thus, this compartment would have a role on redirecting vesicles from the PVC/MVB, which are destined to the LV but have been transported to the cell surface. In the presence of the cell wall, the vesicles would receive a yet unidentified signal from this compartment and their content would be sent to the lytic vacuole directly or through the endocytic pathway.

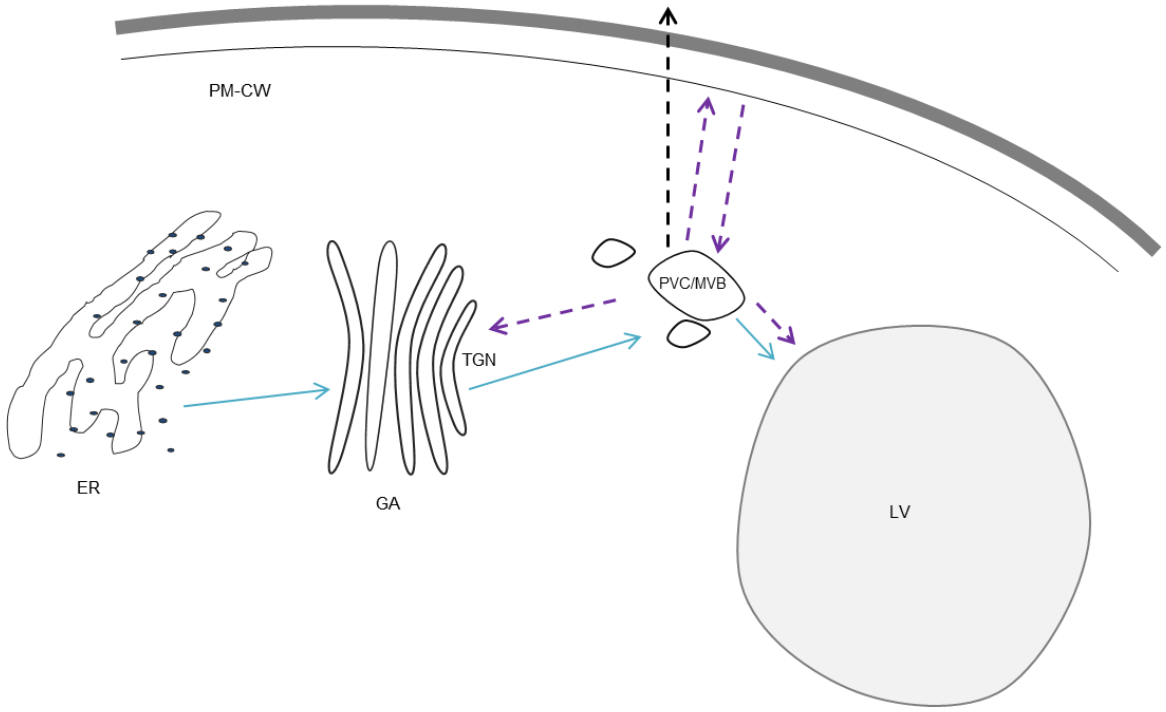

Figure 20 - Schematic representation of the cell wall influence in the sorting of cardosins. The blue arrows represent the classical route followed by cardosins, from the endoplasmic reticulum (ER) to the lytic vacuole (LV), through the Golgi apparatus (GA), trans-Golgi network (TGN) and the prevacuolar compartment/multivesicular body (PVC/MVB). The secretory and endocytic pathways intersect at the PVC/MVB, compartment which mediates the cargo transport between the TGN, the LV and the plasma membrane (PM). According to the results here obtained, proteins destined to the LV could be transported to the cell periphery, by missorting of cargo at the PVC/MVB level. In the presence of the cell wall (CW), the content of the PVC/MVB vesicles would be sent back to the LV through the endocytic pathway (broken purple arrows). In the absence of the CW, the content of the vesicles would be secreted (broken black arrow), as the pathways represented by the broken arrows would not be accessible, for lack of regulation from the CW.

It is currently proposed that the biosynthetic and endocytic pathways may in fact have compartments in common (Samaj et al. 2005) (Fig 21). The TGN is considered to function as an early endosome, mediating the sorting of, not only proteins from the biosynthetic pathways, but also cargo that has been endocytosed from the plasma membrane, for recycling or degradation in the lytic vacuole. The PVC/MVB/late endosome is also a common link of the biosynthetic and endocytic routes, mediating the cargo transport between the TGN, the plasma membrane and the lytic vacuole. Several proteins are known to recycle continuously between the PM and the TGN, namely PM proteins such as the PIN1, PIN2 or AUX1 (Otegui & Spitzer 2008).

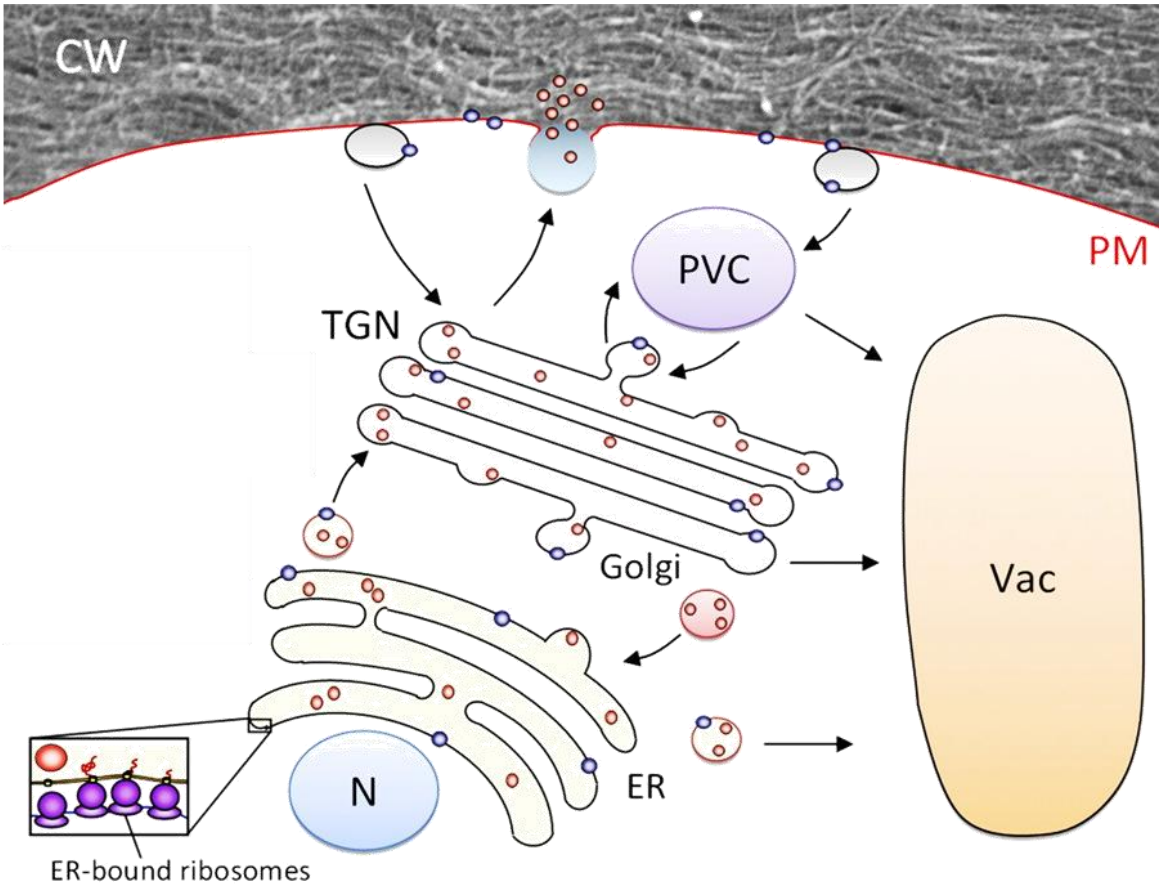

Figure 21 - Schematic representation of the close proximity between the secretory and endocytic pathways. The secretory pathway is represented by the endoplasmic reticulum (ER), the Golgi-apparatus, the trans-Golgi network (TGN), the prevacuolar compartment (PVC) and the vacuole (Vac). Endo and exocytosis events are represented in the plasma membrane/cell wall complex (PM and CW). The TGN is considered to function as an early endosome and the PVC, indistinguishable from the multivesicular body, functions as a late endosome. The arrows represent the multiplicity of cargo routes known to exist between compartments. Adapted from Rose & Lee 2010.

Although it is yet to be clear-cut, as the PVC/MVB functions as a bridge between the plasma membrane and the lytic vacuole, it is not surprising if the two routes interfere with each other and cargo exchanges might actually occur (Park & Jürgens 2011). It was reported in *N. tabacum* cell suspension cultures that enzymes localised in the lytic vacuole were also found in the cell wall and culture medium (Kunze et al. 1998) and it was described that alterations in the intracellular or extracellular conditions, such as modifications in PM/CW complex receptors might in fact lead to missorting of cargo (Baldassarre et al. 2000).

According to the results obtained in the present study for cardosin A and cardosin B in *N. tabacum* protoplasts, we propose a role for the cell wall in the regulation of protein transport in the bridge between the biosynthetic and endocytic pathways. Hence, the cell wall would intercede on the mistargeting of cargo which is actually destined for the vacuole, but yet is erratically transported for the cell surface. The cell wall would then have a role on the redirection of PVC/MVB cargo vesicles that got entangled on the thin interface between biosynthetic and endocytic pathways. Reaching the cell wall, the mistargeted cargo is presumably recycled back to the TGN through the endocytic pathway, in route to the lytic vacuole. During protoplast isolation, the cell wall is enzymatically extracted and so, the regulation of missorting to the cell periphery cesses to exist. Thus, although the major part of the cargo actually reaches the vacuole, some mistargeting might take place, which would lead to the loss of protein through secretion, as it would not suffer from the stimuli to return to the vacuole, where it belonged. It is actually not surprising that the cell wall could regulate important cargo transport events. Many essential roles regarding protein targeting regulation have been reported to be related to the cell wall. An obvious example is the highly regulated transport of cell wall material, such as matrix polysaccharides and cellulose synthase complexes, to the cell periphery (Leucci et al. 2007; De Caroli et al. 2011). It was also demonstrated that the positioning of PIN proteins, which are associated to the plasma membrane and have a role on auxin transport, relies on the integrity of the cell wall (Boutté et al. 2006), which implies some form of regulation of the process by this compartment.

The C-terminal VSD is responsible for cardosins secretion during protoplasting

The C-terminal is a vacuolar sorting determinant conserved among APs (Ramalho-Santos et al. 1998) and so, to investigate if this region influences the sorting of cardosins in the absence/presence of the cell wall, secretion assays were also performed for the C-terminals of both cardosins fused to mCherry. Similarly to the previous assays, at the determined time points (0, 4, 8, 24 and 30 hours) the transformed protoplasts were observed by confocal microscopy and samples were taken from the culture, separating the cells from

the medium for further biochemical analysis. At the same time, the leaves from which the protoplasts were isolated were also observed through CLSM, as an expression control. Burst controls were performed for both C-terminals, using an antibody raised against calreticulin, an ER resident protein, and no burst was detected.

As expected, the mCherry fused to the C-terminal of both cardosins accumulated in the lytic vacuole in *N. tabacum* leaves. In protoplasts though, the constructs were partially secreted, in a similar pattern to the observed for the whole proteins. In fact, it has been demonstrated that this VSD directs cardosins to the vacuole, through the Golgi apparatus, following the classical pathway of soluble proteins. It was also demonstrated that, even so cardosins own two distinct VSDs that might follow different pathways, when both are present in the protein, the C-terminal action is dominant over the PSI's (Pereira et al. 2012, submitted). Therefore, it is not surprising that the C-terminals show the same pattern of partial secretion as for cardosin A and cardosin B. Reaching out from the TGN, the mCherry fused to the C-terminal peptides are transported through PVC/MVB vesicles to the lytic vacuole. However, as the PVC/MVB functions as a bridge between the vacuole and the PM, the cargo may be missorted to the cell periphery. Hence, as in protoplasts the cell wall is absent and so is its regulation over missorting, the mistargeted proteins are lost to the culture medium, as discussed before.

The PSI:mCherry constructs are not secreted upon protoplasting

The PSI domain also acts as a VSD for cardosin A and cardosin B. Despite their co-existence with the C-terminal VSD, which is dominant over the PSI, this domain has shown to correctly direct proteins to the vacuole on its own. The PSI domain action is thought to be tissue or developmental stage specific; however its trigger is still unclear. Recently, the PSIs from cardosins A and B were shown to follow different intracellular routes towards the vacuole. Cardosin A PSI bypasses the Golgi, while cardosin B PSI gets retained in the ER if ER to Golgi transported is blocked (Pereira et al. 2012, submitted). Henceforth, as a way of understanding the influence of the PSI domain of each cardosin in vacuole sorting during protoplasting and cell wall regeneration, secretion assays were performed, in a similar way as for the other constructs. At the established time points (0, 4, 8, 24, 30 hours), the protoplasts were observed through CLSM and protein samples were collected from cells and culture medium separately, for further biochemical analysis. Simultaneously, the leaves from which the protoplasts were isolated were also observed through confocal microscopy at the same time points, as an expression control. Burst controls were performed for PSI A and B, using an antibody raised against calreticulin, an ER resident protein, and no burst was detected.

In leaves, as in protoplasts, both PSIs were mostly accumulated in the vacuole. A slight secretion is detected for PSI A and B, although the secretion detected for the PSI of cardosin A is limited to the 8 and 24 h time points, which is an uncommon pattern for a secretion assay. The strong bands observed in the Western blot might have been due to a different factor rather than secretion, such as a problem during protein extraction. Results from our lab have shown that the PSI from cardosin A follows a route to the lytic vacuole that bypasses the Golgi in a COPII independent manner. The pathway followed by PSI A is also thought not to include the PVC/MVB (Pereira et al. 2012, submitted). Thus, bypassing the Golgi, TGN and PVC/MVB, the PSI from cardosin A will not pass through the interface between the biosynthetic and endocytic pathways. Presumably, when bypassing the Golgi and PVC/MVB, missorting will not occur, which might explain the absence of secretion observed for cardosin A PSI. The PSI from cardosin B, on the other hand, is thought to follow a Golgi-dependent route to the vacuole, presumably due to its glycosylation site, similarly to the described for other APs, such as phytepsin (Törmäkangas et al. 2001; Pereira et al. 2012, submitted). The PSI region, unlike the C-terminal peptides, is known to interact with membranes rather than specific receptors; hence it seems unlikely that the PSI regions would be affected by mistargeting at the PVC/MVB or cell wall regulation. Hence, further studies are needed for a better understanding of cardosin B maturation process in order to better understand the regulation of its sorting.

4.2. Unveiling the role of the PSI domain in the regulation of cardosin A trafficking

The PSI of cardosin A has shown to possess intriguing individualities. In the flower of cardoon, during pollination, cardosin A is thought to travel to the cell wall in order to connect with a pollen receptor. The interaction of the PSI A with biological membranes has already been demonstrated *in vitro* and cardosin A has been detected in the plasma membrane/cell wall complex in cardoon seeds (Egas et al. 2000; Pereira et al. 2008). As a way of better understanding the timing and importance of the cardosin A PSI interaction with membranes, as well as the protein maturation, mutations were planned to impair the cleavage sites of the PSI domain of cardosin A. This approach has already been tried before however the impairment of the PSI cleavage was not successful (Silva 2009, Master Thesis). In an attempt to improve the chance of success, collaboration was established with the Theoretical Chemistry Group of the Faculty of Chemistry in Porto University. Thus, using modulation homology with available crystallographic structures of other APs, such as prophytepsin, it was observed that the PSI domain creates a flexible loop. Henceforth, as any mutations

performed on the cleavage sites of the PSI would not affect the integrity of the structure, drastic mutations in the aminoacidic sequence were planned with the help of Theoretical Chemistry Group and subsequently executed by site-directed mutagenesis. Two constructions were made with the planned mutations; one linked to the fluorescent protein mCherry (AmutPSICh – to allow analysis through CLSM) and the other without mCherry (AmutPSI – to allow the analysis of protein processing through Western blotting). The results obtained by CLSM for AmutPSICh showed low expression when compared to the non-mutated cardosin A. The mutant protein was observed accumulating in the lytic vacuole when 3 and 6 days had passed since infiltration; however, in a much lower extent when compared to cardosin A. Round-shaped compartments were also detected at the third and sixth days after infiltration, which appear to be protein accumulation in the ER, probably due to protein incorrect folding. However, co-localisation studies are needed in order to fully understand the accumulation patterns of AmutPSICh. As for AmutPSI, the aim was to confirm by Western blotting that the cleavage of the PSI domain had in fact been impaired. The Western blotting for AmutPSI could not be performed in due time. In light of the results obtained so far, the PSI processing blockage seems to slow protein transport to the vacuole, but does not completely impair, as fluorescent signal is clear in this organelle. However, the analysis of AmutPSI will be essential to draw any final conclusions regarding the observations made for AmutPSICh and is a near future priority.

5. Conclusions and Future Perspectives

Taking together the data obtained during this study, the hypothesis of an unknown form of regulation of protein transport by the cell wall seems plausible. The absence of the cell wall in *N. tabacum* protoplasts originates a partial secretion of cardosin A and B to the culture medium. The same pattern is observed for C-terminal peptides, which work as VSDs for cardosins and other APs, although no secretion is observed for the PSI of cardosin A. The results observed for the PSI A are most likely due to the different intracellular pathway followed by this domain, when compared to cardosins and C-terminal peptides, bypassing the Golgi apparatus and the PVC/MVB in its route to the lytic vacuole. As for the PSI of cardosin B, further studies on the maturation of the protein and its intracellular route are yet needed for a full understanding of the results here obtained.

Despite the fact that interesting observations were possible during the secretion assays, further optimisations are necessary regarding the timing of cell wall regeneration process, as it would be important to give the cells more time to totally regenerate a new cell wall. The monitorisation of the newly formed wall could also be improved by co-transformation of cardosins with a cell wall fluorescent marker. Moreover, as a way of confirming the protein secretion, co-transformation of cardosins with internal controls could be performed. Another future aim is to perform the same experiments with other known vacuolar proteins, as a way of understanding if the proteins' transport regulation from the cell wall is unique among cardosins or a common protein sorting control.

Furthermore, the confirmation of the hypothesised intracellular routes should involve the study and interaction of cardosins with specific vacuolar receptors, such as BP80. Co-transformation of cardosins with dominant negative mutants of vacuolar receptors, as well as the use of drugs affecting vesicular and endocytic trafficking (wortmaninn or concamycin A, for example) will be of utmost importance in the definition of cardosins sorting routes. The vacuolar receptors could also be tracked using fusions with photoconvertible proteins.

Regarding the experimental system, the transient expression of *N. tabacum* is somewhat limited and so it would be interesting to perform the same experiments in a stable expression system. Comparison between leaf and cellular systems would also be interesting, and the use of BY-2 cell suspensions expressing both cardosins (already available in our lab) seems to be a good model.

The proposed mutations on the cleavage sites of the PSI domain from cardosin A were successfully executed. The induced mutations showed to affect protein trafficking to the vacuole; however, the analysis of AmutPSI by Western blotting will be essential to confirm if

the removal of the PSI domain during processing was actually impaired. Co-localisation studies with internal controls such as GFP-HDEL will be performed, as a way of confirming the ER-accumulation of the protein aggregates observed through confocal microscopy. Further studies involving blocking of trafficking between specific compartments may be necessary to understand the influence of the mutations on the PSI domain cleavage sites in the intracellular sorting of cardosin A. Later on, secretion assays will be performed so as to unveil the influence of PSI cleavage impairment on cell wall regulation of cardosin A sorting.

As a whole, the data obtained during this dissertation points to a putative role for the cell wall in the regulation of vacuolar sorting. Moreover, by suggesting a working model of such regulation on cardosins trafficking, this study provides the basis for further discoveries on the cell wall as a putatively dynamic and active participant on the regulation of intracellular sorting of proteins in general.

6. BIBLIOGRAPHIC REFERENCES

Baldassarre, M. et al., 2000. Regulation of protein sorting at the TGN by plasma membrane receptor activation. *Journal of cell science*, 113 Pt 4, pp.741–8.

Balestri, E. & Cinelli, F., 2001. Isolation and cell wall regeneration of protoplasts from *Posidonia oceanica* and *Cymodocea nodosa*. *Aquatic Botany*, 70(3), pp.237–242.

Boutté, Y. et al., 2006. The plasma membrane recycling pathway and cell polarity in plants: studies on PIN proteins. *Journal of cell science*, 119(Pt 7), pp.1255–65.

Brandizzi, F & Snapp, E., 2002. Membrane protein transport between the endoplasmic reticulum and the Golgi in tobacco leaves is energy dependent but cytoskeleton independent: evidence from. *The Plant Cell* 24(2), pp.108–17.

Cai, H., Reinisch, K. & Ferro-Novick, S., 2007. Coats, tethers, Rabs, and SNAREs work together to mediate the intracellular destination of a transport vesicle. *Developmental cell*, 12(5), pp.671–82.

De Caroli, M. et al., 2011. Dynamic protein trafficking to the cell wall. *Plant Signaling & Behavior*, 6(7), pp.1012–1015.

Carter, C.J., Bednarek, S.Y. & Raikhel, N.V., 2004. Membrane trafficking in plants: new discoveries and approaches. *Current opinion in plant biology*, 7(6), pp.701–7.

Cordeiro, M.C. et al., 1994. Isolation and characterization of a cDNA from flowers of *Cynara cardunculus* encoding cyprosin (an aspartic proteinase) and its use to study the organ-specific expression of cyprosin. *Plant Molecular Biology*, 24(5), pp.733–741.

da Costa, D.S. et al., 2010. Dissecting cardosin B trafficking pathways in heterologous systems. *Planta*, 232(6), pp.1517–30.

Denecke, J et al., 1995. The tobacco homolog of mammalian calreticulin is present in protein complexes in vivo. *The Plant cell*, 7(4), pp.391–406.

Denecke, J, Botterman, J. & Deblaere, R., 1990. Protein secretion in plant cells can occur via a default pathway. *The Plant cell*, 2(1), pp.51–9.

Denecke, J. et al., 2012. Secretory Pathway Research: The More Experimental Systems the Better. *The Plant Cell,* 24(4):1316-26.

Duarte, P., Pissarra, José & Moore, I., 2008. Processing and trafficking of a single isoform of the aspartic proteinase cardosin A on the vacuolar pathway. *Planta*, 227(6), pp.1255–68.

Egas, C. et al., 2000. The saposin-like domain of the plant aspartic proteinase precursor is a potent inducer of vesicle leakage. *The Journal of biological chemistry*, 275(49), pp.38190–6.

Faraco, M. et al., 2011. One protoplast is not the other! *Plant physiology*, 156(2), pp.474–8.

Faro, C. et al., 1999. Cloning and characterization of cDNA encoding cardosin A, an RGD-containing plant aspartic proteinase. *The Journal of biological chemistry*, 274(40), pp.28724–9.

Figueiredo, R. et al., 2006. The embryo sac of *Cynara cardunculus:* ultrastructure of the development and localisation of the aspartic proteinase cardosin B. *Sexual Plant Reproduction*, 19(2), pp.93–101.

Foresti, O. & Denecke, Jürgen, 2008. Intermediate organelles of the plant secretory pathway: identity and function. *Traffic (Copenhagen, Denmark)*, 9(10), pp.1599–612.

Hahne, G., Herth, W. & Hoffmann, F., 1983. Wall formation and cell division in fluorescence-labelled plant protoplasts. *Protoplasma*, 115(2-3), pp.217–221.

Hanton, S.L. et al., 2005. Crossing the divide--transport between the endoplasmic reticulum and Golgi apparatus in plants. *Traffic (Copenhagen, Denmark)*, 6(4), pp.267–77.

Hanton, S.L., Matheson, L. a & Brandizzi, Federica, 2006. Seeking a way out: export of proteins from the plant endoplasmic reticulum. *Trends in plant science*, 11(7), pp.335–43.

Hawes, Chris & Satiat-Jeunemaitre, Béatrice, 2005. The plant Golgi apparatus--going with the flow. *Biochimica et biophysica acta*, 1744(2), pp.93–107.

Horine, R.K. & Ruesink, a W., 1972. Cell Wall Regeneration around Protoplasts Isolated from Convolvulus Tissue Culture. *Plant physiology*, 50(4), pp.438–45.

Jolliffe, N. a, Craddock, C.P. & Frigerio, L., 2005. Pathways for protein transport to seed storage vacuoles. *Biochemical Society transactions*, 33(Pt 5), pp.1016–8.

Jurgens, G., 2004. Membrane trafficking in plants. *Annual review of cell and developmental biology*, 20, pp.481–504.

Kang, B.-H. et al., 2011. Electron tomography of RabA4b- and PI-4Kβ1-labeled trans Golgi network compartments in Arabidopsis. *Traffic (Copenhagen, Denmark)*, 12(3), pp.313–29.

Kervinen, J. et al., 1999. Crystal structure of plant aspartic proteinase prophytepsin: inactivation and vacuolar targeting. *The EMBO journal*, 18(14), pp.3947–55.

Kunze, I. et al., 1998. Evidence for secretion of vacuolar alpha-mannosidase, class I chitinase, and class I beta-1,3-glucanase in suspension cultures of tobacco cells. *Planta*, 205(1), pp.92–9.

Leucci, M.R. et al., 2007. Secretion marker proteins and cell-wall polysaccharides move through different secretory pathways. *Planta*, 225(4), pp.1001–17.

Martinoia, E., Maeshima, M. & Neuhaus, H.E., 2007. Vacuolar transporters and their essential role in plant metabolism. *Journal of experimental botany*, 58(1), pp.83–102. Marty, F., 1999. Plant vacuoles. *The Plant Cell Online*, 11(April), pp.587–599.

Matheson, L. a, Hanton, S.L. & Brandizzi, Federica, 2006. Traffic between the plant endoplasmic reticulum and Golgi apparatus: to the Golgi and beyond. *Current opinion in plant biology*, 9(6), pp.601–9.

Mazorra-Manzano, M.A. et al., 2010. Structure-function characterization of the recombinant aspartic proteinase A1 from Arabidopsis thaliana. *Phytochemistry*, 71(5-6), pp.515–23.

Müller, J. et al., 2007. Molecular dissection of endosomal compartments in plants. *Plant physiology*, 145(2), pp.293–304.

Nagata, T. & Takebe, I., 1971. Plating of isolated tobacco mesophyll protoplasts on agar medium. *Planta*, 99(1), pp.12–20.

Nebenführ, a & Staehelin, L. a, 2001. Mobile factories: Golgi dynamics in plant cells. *Trends in plant science*, 6(4), pp.160–7.

Nebenführ, A., 2002. Vesicle traffic in the endomembrane system: a tale of COPs, Rabs and SNAREs. *Current Opinion in Plant Biology*, 5(6), pp.507–512.

Neuhaus, J.M. & Rogers, J.C., 1998. Sorting of proteins to vacuoles in plant cells. *Plant molecular biology*, 38(1-2), pp.127–44.

Nickel, W. & Rabouille, C., 2009. Mechanisms of regulated unconventional protein secretion. *Nature reviews. Molecular cell biology*, 10(2), pp.148–55.

Nickel, W. & Seedorf, M., 2008. Unconventional mechanisms of protein transport to the cell surface of eukaryotic cells. *Annual review of cell and developmental biology*, 24, pp.287–308.

Otegui, M.S. & Spitzer, C., 2008. Endosomal functions in plants. *Traffic (Copenhagen, Denmark)*, 9(10), pp.1589–98.

Paris, N. et al., 1996. Plant cells contain two functionally distinct vacuolar compartments. *Cell*, 85(4), pp.563–72.

Park, M. & Jürgens, G., 2011. Membrane traffic and fusion at post-Golgi compartments. *Frontiers in plant science*, 2(January), p.111.

Pereira, C.S. et al., 2008. Cardosins in postembryonic development of cardoon: towards an elucidation of the biological function of plant aspartic proteinases. *Protoplasma*, 232(3-4), pp.203–213.

Pereira, Cláudia et al., 2012. Characterization of two new vacuolar sorting signals uncovers different vacuolar routes. *Molecular plant - under revision*, pp.1–33.

Pissarra, José, Pereira, Claudia, Soares, D., et al., 2007. From Flower to Seed Germination in Cynara cardunculus: A Role for Aspartic Proteinases. *Internation Journal of Plant Developmental Biology*, 1(2), pp.274–281.

Pissarra, José, Pereira, Claudia, Costa, D.S. da, et al., 2007. From Flower to Seed Germination in *Cynara cardunculus*: A Role for Aspartic Proteinases. *Internation Journal of Plant Developmental Biology*, pp.274–281.

Ramalho-Santos, M. et al., 1997a. Cardosin A, an abundant aspartic proteinase, accumulates in protein storage vacuoles in the stigmatic papillae of Cynara cardunculus L. *Planta*, 203(2), pp.204–12.

Ramalho-Santos, M. et al., 1997b. Cardosin A, an abundant aspartic proteinase, accumulates in protein storage vacuoles in the stigmatic papillae of Cynara cardunculus L. *Planta*, 203(2), pp.204–12.

Ramalho-Santos, M. et al., 1998. Identification and proteolytic processing of procardosin A. *European journal of biochemistry / FEBS*, 255(1), pp.133–8.

Richter, S., Voss, U. & Jürgens, G., 2009. Post-Golgi traffic in plants. *Traffic (Copenhagen, Denmark)*, 10(7), pp.819–28.

Robinson, David G, Jiang, L. & Schumacher, K., 2008. The endosomal system of plants: charting new and familiar territories. *Plant physiology*, 147(4), pp.1482–92.

Robinson, David G & Schlösser, U.G., 1978. Cell wall regeneration by protoplasts of Chlamydomonas. *Planta*, 141(1), pp.83–92.

Rojo, E. & Denecke, Jurgen, 2008. What is moving in the secretory pathway of plants? *Plant physiology*, 147(4), pp.1493–503.

Rose, J.K.C. & Lee, S.-J., 2010. Straying off the highway: trafficking of secreted plant proteins and complexity in the plant cell wall proteome. *Plant physiology*, 153(2), pp.433–6.

Samaj, J. et al., 2005. The endocytic network in plants. *Trends in cell biology*, 15(8), pp.425–33.

Satiat-Jeunemaitre, B, Boevink, P. & Hawes, C, 1999. Membrane trafficking in higher plant cells: GFP and antibodies, partners for probing the secretory pathway. *Biochimie*, 81(6), pp.597–605.

Silva, N., 2009. *Mutantes de cardosinas para o estudo do Plant Specific Insert*. Faculty of Sciences - University of Porto.

Szymanski, D.B. & Cosgrove, D.J., 2009. Dynamic coordination of cytoskeletal and cell wall systems during plant cell morphogenesis. *Current biology : CB*, 19(17), pp.R800–11.

Tse, Y. et al., 2004. Identification of multivesicular bodies as prevacuolar compartments in Nicotiana tabacum BY-2 cells. *The Plant Cell*, 16(March), pp.672–693.

Törmäkangas, K. et al., 2001. A vacuolar sorting domain may also influence the way in which proteins leave the endoplasmic reticulum. *The Plant cell*, 13(9), pp.2021–32.

Veríssimo, P. et al., 1996. Purification, characterization and partial amino acid sequencing of two new aspartic proteinases from fresh flowers of *Cynara cardunculus* L. *European journal of biochemistry / FEBS*, 235(3), pp.762–8.

Vieira, M. et al., 2001. Molecular cloning and characterization of cDNA encoding cardosin B, an aspartic proteinase accumulating extracellularly in the transmitting tissue of *Cynara cardunculus* L. *Plant molecular biology*, 45(5), pp.529–39.

Vitale, a & Raikhel, N., 1999. What do proteins need to reach different vacuoles? *Trends in plant science*, 4(4), pp.149–155.

Vitale, A & Denecke, J, 1999. The endoplasmic reticulum-gateway of the secretory pathway. *The Plant cell*, 11(4), pp.615–28.

Vitale, Alessandro & Ceriotti, A., 2004. Protein quality control mechanisms and protein storage in the endoplasmic reticulum. A conflict of interests? *Plant physiology*, 136(3), pp.3420–6.

Wightman, R. & Turner, S., 2010. Trafficking of the plant cellulose synthase complex. *Plant physiology*, 153(2), pp.427–32.